AD-A153 111 BASIC EMC TECHNOLOGY ADVANCEMENT FOR C3 SYSTEMS VOLUME 1/2
4F PREDICTION OF C.. (U) SOUTHEASTERN CENTER FOR
ELECTRICAL ENGINEERING EDUCATION INC S..
UNCLASSIFIED W E BEECH ET AL. DEC 84 F/G 9/3 NL

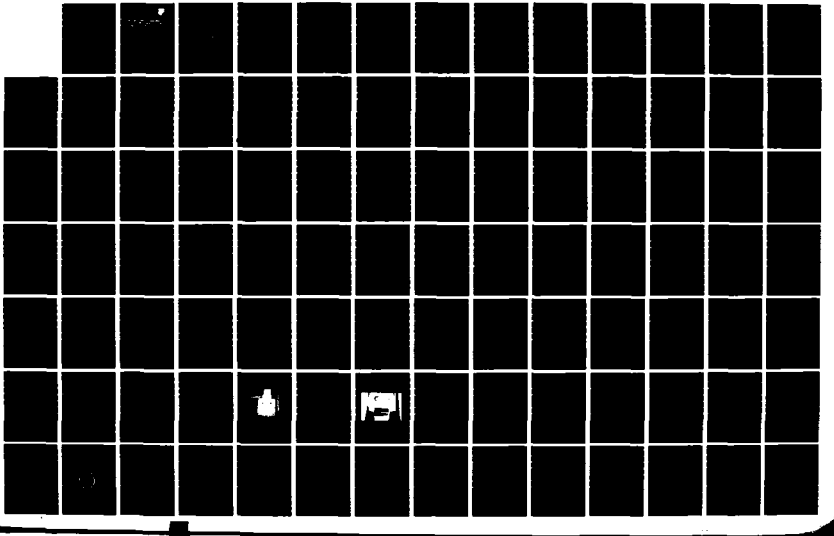

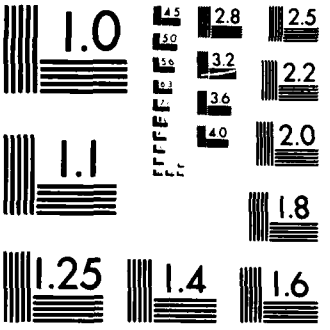

MICROCOPY RESOLUTION TEST CHART
NATIONAL BUREAU OF STANDARDS-1963-A

RADC-TR-82-286, Vol IVf (of six)
Final Technical Report
December 1984

AD-A153 111

BASIC EMC TECHNOLOGY ADVANCEMENT FOR C³ SYSTEMS - Prediction of Crosstalk in Flatpack Coaxial Cables

Southeastern Center for Electrical Engineering Education

Wayne E. Beech and Clayton R. Paul

APPROVED FOR PUBLIC RELEASE; DISTRIBUTION UNLIMITED

DTIC
ELECTE
MAY 2 1985
S D
A

FILE COPY

ROME AIR DEVELOPMENT CENTER
Air Force Systems Command
Griffiss Air Force Base, NY 13441-5700

85 04 30 024

This report has been reviewed by the RADC Public Affairs Office (PA) and is releasable to the National Technical Information Service (NTIS). At NTIS it will be releasable to the general public, including foreign nations.

RADC-TR-82-286, Volume IVf (of six) has been reviewed and is approved for publication.

APPROVED: Roy F. Stratton

ROY F. STRATTON
Project Engineer

APPROVED:

W. S. TUTHILL, Colonel, USAF
Chief, Reliability & Compatibility Division

FOR THE COMMANDER:

JOHN A. RITZ
Acting Chief, Plans Office

If your address has changed or if you wish to be removed from the RADC mailing list, or if the addressee is no longer employed by your organization, please notify RADC (RBCT) Griffiss AFB NY 13441-5700. This will assist us in maintaining a current mailing list.

Do not return copies of this report unless contractual obligations or notices on a specific document requires that it be returned.

UNCLASSIFIED
SECURITY CLASSIFICATION OF THIS PAGE

REPORT DOCUMENTATION PAGE

1a. REPORT SECURITY CLASSIFICATION UNCLASSIFIED	1b. RESTRICTIVE MARKINGS N/A
2a. SECURITY CLASSIFICATION AUTHORITY N/A	3. DISTRIBUTION/AVAILABILITY OF REPORT Approved for public release; distribution unlimited.
2b. DECLASSIFICATION/DOWNGRADING SCHEDULE N/A	
4. PERFORMING ORGANIZATION REPORT NUMBER(S) N/A	5. MONITORING ORGANIZATION REPORT NUMBER(S) RADC-TR-82-286, Vol IVf (of six)
6a. NAME OF PERFORMING ORGANIZATION Southeastern Center for Electrical Engineering Education 6b. OFFICE SYMBOL (If applicable)	7a. NAME OF MONITORING ORGANIZATION Rome Air Development Center (RBCT)
6c. ADDRESS (City, State and ZIP Code) 1101 Massachusetts Avenue St. Cloud FL 32706	7b. ADDRESS (City, State and ZIP Code) Griffiss AFB NY 13441-5700
8a. NAME OF FUNDING/SPONSORING ORGANIZATION Rome Air Development Center 8b. OFFICE SYMBOL (If applicable) RBCT	9. PROCUREMENT INSTRUMENT IDENTIFICATION NUMBER F30602-81-C-0062
8c. ADDRESS (City, State and ZIP Code) Griffiss AFB NY 13441-5700	10. SOURCE OF FUNDING NOS. PROGRAM ELEMENT NO.: 62702F; PROJECT NO.: 2338; TASK NO.: 03; WORK UNIT NO: 35

11. TITLE (Include Security Classification) BASIC EMC TECHNOLOGY ADVANCEMENT FOR C^3 SYSTEMS - Prediction of Crosstalk in Flatpack Coaxial Cables

12. PERSONAL AUTHOR(S)
Wayne E. Beech, Clayton R. Paul

13a. TYPE OF REPORT	13b. TIME COVERED	14. DATE OF REPORT (Yr., Mo., Day)	15. PAGE COUNT
Final	FROM Sep 82 TO Dec 83	December 1984	114

16. SUPPLEMENTARY NOTATION
Work was performed at University of Kentucky, Lexington, KY 40506
Project Engineers: Gerald Capraro and Roy F. Stratton

17 COSATI CODES		
FIELD	GROUP	SUB. GR.
09	03	
17	02	1

18. SUBJECT TERMS (Continue on reverse if necessary and identify by block number)
Crosstalk, Electromagnetic Compatibility, Flatpack Cables, Transmission LINES, ... Modelling

19. ABSTRACT (Continue on reverse if necessary and identify by block number)

The electromagnetic crosstalk present in a class of cables known as flatpack, coaxial cables is investigated. The multiconductor transmission line equations are used to derive a model of a general flatpack, coaxial cable consisting of n cables. This model is then implemented as a digital computer program to allow simulation of the crosstalk levels present in the cable. This simulation is compared to experimental results to prove that the model is valid and can accurately predict the crosstalk levels. Also the effect of common impedance coupling, the presence of drain wires to allow for connection to the shields of the cable, and the presence of pigtail sections (exposed sections of wire) is examined to determine their effect on the overall electromagnetic crosstalk present in the cable.

20. DISTRIBUTION/AVAILABILITY OF ABSTRACT UNCLASSIFIED/UNLIMITED ☒ SAME AS RPT ☐ DTIC USERS ☐	21. ABSTRACT SECURITY CLASSIFICATION UNCLASSIFIED
22a. NAME OF RESPONSIBLE INDIVIDUAL ROY F. STRATTON	22b. TELEPHONE NUMBER (Include Area Code) (315) 330-2563 22c. OFFICE SYMBOL RADC (RBCT)

DD FORM 1473, 83 APR EDITION OF 1 JAN 73 IS OBSOLETE

UNCLASSIFIED
SECURITY CLASSIFICATION OF THIS PAGE

TABLE OF CONTENTS

NOTE: Qualified requesters may obtain copies of Chapters 4, 5, and Appendices A & B by contacting Roy Stratton RADC (RBCT) Griffiss AFB NY 13441-5700, phone 315-330-2563 or Autovon 8-587-2563

DTIC COPY INSPECTED 1

A1

CHAPTER 1

INTRODUCTION

Many different line types and configurations, such as twisted pairs, coaxial cables, and shielded twisted pairs, have been used in the past to reduce the amount of electromagnetic crosstalk between two or more circuits which are in close proximity to each other. A relatively new type of cable that is being used is the flatpack, coaxial cable. This type of cable is used to reduce crosstalk in cables which interconnect peripherals in many high-speed digital computer systems. The flatpack, coaxial cable, shown in Figure 1.1, consists of n coaxial cables that are bonded together to form a flat, linear array of individual coaxial cables.

It is generally assumed that coaxial cables, as well as the other types of cables mentioned above, provide a degree of protection from electromagnetic crosstalk that is greater than unshielded, straight wire. This assumption is not as obvious or as valid as one would think. The degree of protection provided by any type of cable can greatly depend on factors that one might not consider; for instance, load impedances and their configuration, thickness of shields, frequency of operation, presence of pigtail sections, etc. can greatly affect the amount of protection

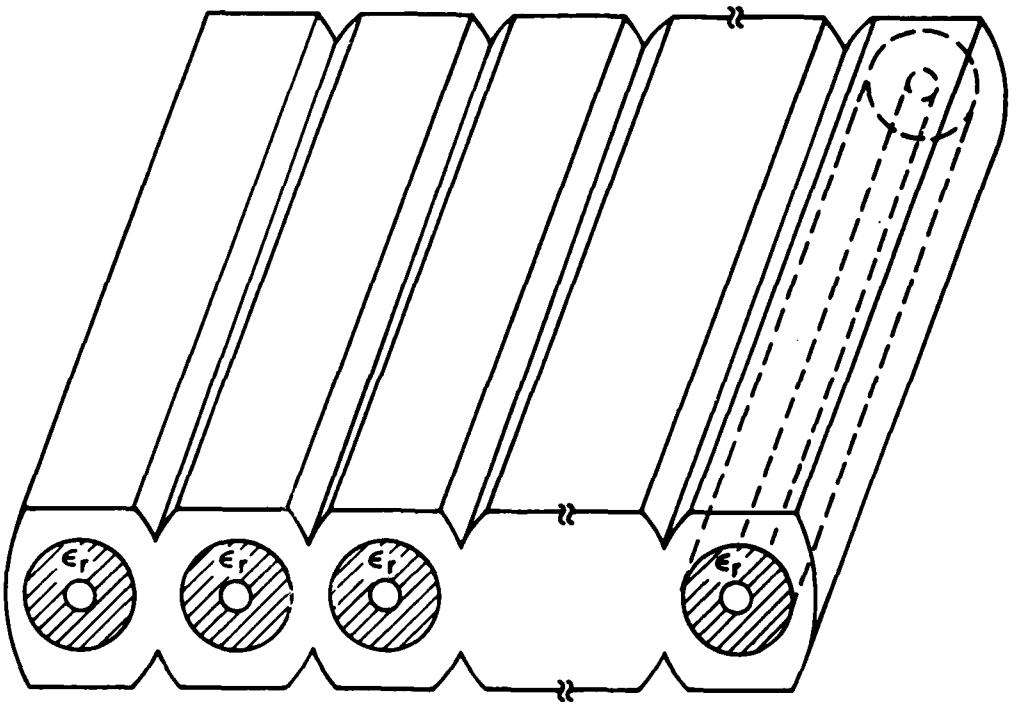

Figure 1.1 - The Flatpack, Coaxial Cable.

given.

The distributed parameter, transmission line equations have been used to accurately predict the electromagnetic crosstalk in ribbon cables[1], twisted pairs[2,3], and braided shield cables[4]. It is the intent of this thesis to derive a multiconductor transmission line model of the flatpack, coaxial cable which has pigtail sections at each end of the line to allow for connection to the cables. This model will then be implemented in a digital computer program to allow one to answer the "degree of protection" question for different situations via simulation, thus reducing costly experimental work. Also, the simulation program will show the degradation in protection for a given cable due to the presence of pigtail sections.

In Chapter 2, the transmission line equations and the concept of shield transfer impedance are used to derive a multiconductor transmission line model for both the shielded and pigtail sections of the flatpack, coaxial cable. From this model the chain parameter matrix for the line will be calculated and the terminal conditions incorporated to allow for an unique solution to the levels of crosstalk for a given line configuration.

In Chapter 3, the cable configuration that was used for the experimental work and comparison to the computer results provided by the digital computer program FLATCOAX are shown. Degradation of the overall protection due to the

presence of drain wires over the shielded section will also be discussed. Also a comparison of the actual experimental measurements and the computed results will be shown to display the accuracy which can be obtained by use of the computer simulation and to show how pigtail sections and the presence of the drain wire degrade the overall protection of the flatpack, coaxial cable.

Chapter 4 contains a description of the program FLATCOAX which is used to simulate the crosstalk in the flatpack, coaxial cables. Included is a description of all variables and constants used by the program, a flowchart of the program, and a card-by-card description of the program code.

Chapter 5 will serve as a users manual for the program FLATCOAX. It will show one how to setup and input the line characteristics and terminal conditions for a given cable configuration and how to interpret the output that is created by the program.

In Chapter 6 the conclusions drawn from this study will be presented. It will be shown that common impedance coupling is the dominant contributor to the total crosstalk at the lower frequencies. Also it was found that the presence of drain wires over the shielded section greatly affect the levels of crosstalk present in the flatpack, coaxial cable. It was also found that the presence of

pigtail section (exposed sections of wires) can greatly increase the crosstalk levels at the higher frequencies. Finally, and most importantly, it will be shown that the levels of crosstalk in the flatpack, coaxial cable can be accurately predicted using a digital computer simulation.

CHAPTER 2

THE MULTICONDUCTOR TRANSMISSION LINE MODEL

Any n+1 conductor transmission line, including the flatpack, coaxial cable, can be characterized by a 2n-port network. For the 2n-port network, shown in Figure 2.1, the 2n port variables are the n voltages and n currents at the left end of the port and the n voltages and n currents at the right end of the port. We can write the voltages at the left end of the port, $\underline{V}_L$, in vector form as

$$\underline{V}_L = \begin{bmatrix} V_{L1} \\ V_{L2} \\ \vdots \\ V_{Ln} \end{bmatrix}$$

We can similarly define vectors that represent the voltages at the right end of the port, $\underline{V}_R$, the currents at the left end of the port, $\underline{I}_L$, and the currents at the right end of the port, $\underline{I}_R$, as

$$\underline{V}_R = \begin{bmatrix} V_{R1} \\ V_{R2} \\ \vdots \\ V_{Rn} \end{bmatrix} \qquad \underline{I}_L = \begin{bmatrix} I_{L1} \\ I_{L2} \\ \vdots \\ I_{Ln} \end{bmatrix} \qquad \underline{I}_R = \begin{bmatrix} I_{R1} \\ I_{R2} \\ \vdots \\ I_{Rn} \end{bmatrix}$$

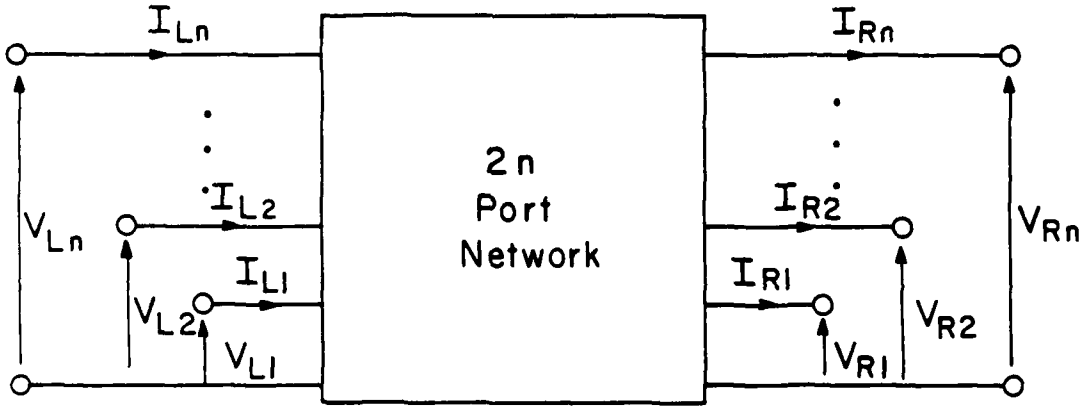

Figure 2.1 - A General 2n-Port Network.

These voltage and current vectors can be used to relate the port parameters at the left end of the port to the port parameters at the right end of the port as follows:

$$\begin{bmatrix} \underline{V}_R \\ \underline{I}_R \end{bmatrix} = \begin{bmatrix} \quad \\ \quad \underset{\sim}{\Phi} \quad \\ \quad \end{bmatrix} \begin{bmatrix} \underline{V}_L \\ \underline{I}_L \end{bmatrix} \tag{2-1}$$

where the 2n x 2n $\underset{\sim}{\Phi}$ matrix is known as the chain parameter matrix and can be broken into four distinct parts

$$\underset{\sim}{\Phi} = \begin{bmatrix} \underset{\sim}{\Phi}_{11} & \underset{\sim}{\Phi}_{12} \\ \underset{\sim}{\Phi}_{21} & \underset{\sim}{\Phi}_{22} \end{bmatrix} \tag{2-2}$$

Each of the $\underset{\sim}{\Phi}_{ij}$ submatrices is n x n and the above port representation becomes

$$\underline{V}_R = \underset{\sim}{\Phi}_{11}\, \underline{V}_L + \underset{\sim}{\Phi}_{12}\, \underline{I}_L \tag{2-3a}$$

$$\underline{I}_R = \underset{\sim}{\Phi}_{21}\, \underline{V}_L + \underset{\sim}{\Phi}_{22}\, \underline{I}_L \tag{2-3b}$$

The above concepts can be used to characterize an n+1 conductor transmission line in the following manner[12]. Consider the general, n+1 conductor, uniform transmission line shown in Figure 2.2(a). For sinusoidal, steady state excitation of the line, and the Transverse ElectroMagnetic mode (TEM) of propagation, it is possible to uniquely define voltages of each conductor, $V_i(x)$, with respect to the reference conductor (the 0^{th} conductor) and conductor currents, $I_i(x)$, as shown in Figure 2.2(b) [12]. These voltages and currents can be related in the limit as $\Delta x \to 0$, via the multiconductor transmission line(MTL) equations:

$$\frac{d\underline{V}(x)}{dx} = -\underset{\sim}{Z}\, \underline{I}(x) \tag{2-4a}$$

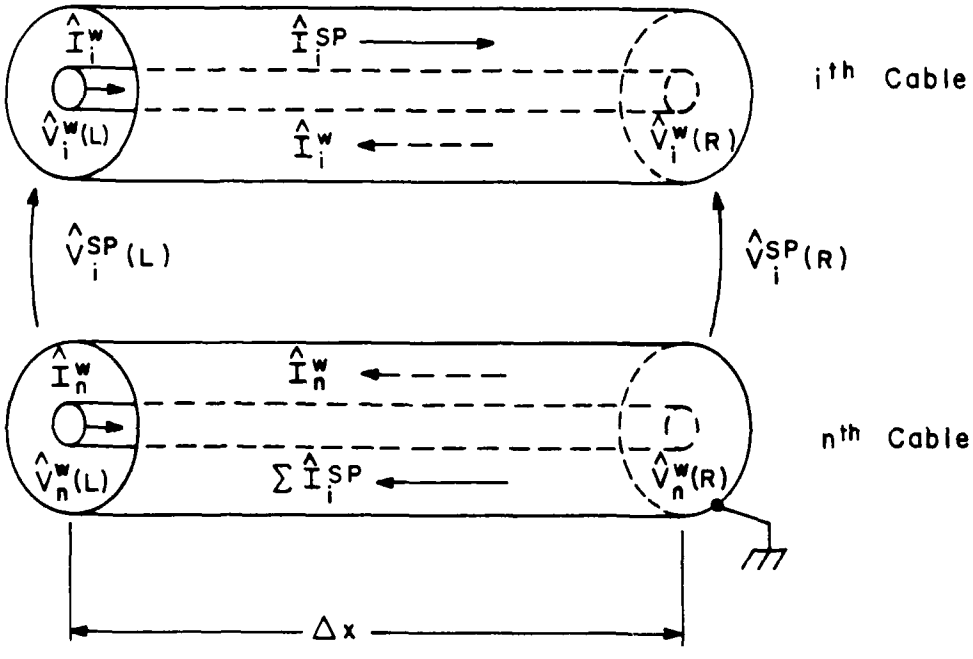

Figure 2.6 - Δx Section of the Shielded Section of the Cable.

$$\begin{bmatrix} \dot{\underline{V}}^{w}(x) \\ \dot{\underline{V}}^{sp}(x) \end{bmatrix} = -(\underset{\sim}{Z}_C + j\omega\underset{\sim}{L}_S) \begin{bmatrix} \underline{I}^{w}(x) \\ \underline{I}^{sp}(x) \end{bmatrix} \quad (2\text{-}18)$$

and

$$\begin{bmatrix} \dot{\underline{I}}^{w}(x) \\ \dot{\underline{I}}^{sp}(x) \end{bmatrix} = -j\omega\underset{\sim}{C}_S \begin{bmatrix} \underline{V}^{w}(x) \\ \underline{V}^{sp}(x) \end{bmatrix} \quad (2\text{-}19)$$

where $\underset{\sim}{Z}_C$, $\underset{\sim}{L}_S$, and $\underset{\sim}{C}_S$ are the per-unit-length conductor impedance matrix, inductance matrix, and capacitance matrix of the shielded section, respectively.

We will first derive the per-unit-length conductor impedance matrix, $\underset{\sim}{Z}_C$, of the shielded section. This can be accomplished by writing loop equations for a Δx section of the line shown in Figure 2.6. First we will write the equation that relates the voltage of the i^{th} wire at the left end of the Δx section to the voltage of the i^{th} wire at the right end of the Δx section($i=1,2,\ldots,n-1$). This equation can be written as

$$\frac{\hat{V}_i^w(R) - \hat{V}_i^w(L)}{\Delta x} = -Z_{con}\,\hat{I}_i^w - Z_{SH}\,\hat{I}_i^w + Z_T\,\hat{I}_i^{sp} \quad (2\text{-}20)$$

where Z_{con} is the impedance of the center conductors of the individual coaxial cables. Since all the shields are identical we can refer to each of the shield transfer impedances as just Z_T and each of the shield impedances as Z_{SH} without any need for distinction.

Next we will write the equation that relates the voltage of the i^{th} shield at the left end of the Δx section to the voltage of the i^{th} shield at the right end of the Δx

the i^{th} shield. The shield currents, I_i^{sp}, are assumed to flow on the outside of the i^{th} shield and return on the reference shield (chosen arbitrarily).

It be will convenient to define voltage and current vectors in the following manner to be used through out the derivations. We will define the total voltage vector, $\underline{V}$, as:

$$\underline{V} = \begin{bmatrix} \underline{V}^w \\ \underline{V}^{sp} \end{bmatrix} \tag{2-16a}$$

where

$$\underline{V}^w = \begin{bmatrix} V_1^w \\ V_2^w \\ \cdot \\ \cdot \\ \cdot \\ V_n^w \end{bmatrix} \quad (2\text{-}16b) \quad \text{and} \quad \underline{V}^{sp} = \begin{bmatrix} V_1^{sp} \\ V_2^{sp} \\ \cdot \\ \cdot \\ \cdot \\ V_n^{sp} \end{bmatrix} \tag{2-16c}$$

and the total current vector, $\underline{I}$, as:

$$\underline{I} = \begin{bmatrix} \underline{I}^w \\ \underline{I}^{sp} \end{bmatrix} \tag{2-17a}$$

where

$$\underline{I}^w = \begin{bmatrix} I_1^w \\ I_2^w \\ \cdot \\ \cdot \\ \cdot \\ I_n^w \end{bmatrix} \quad (2\text{-}17b) \quad \text{and} \quad \underline{I}^{sp} = \begin{bmatrix} I_1^{sp} \\ I_2^{sp} \\ \cdot \\ \cdot \\ \cdot \\ I_n^{sp} \end{bmatrix} \tag{2-17c}$$

The transmission line equations can be written as follows for the shielded section of the cable[12]:

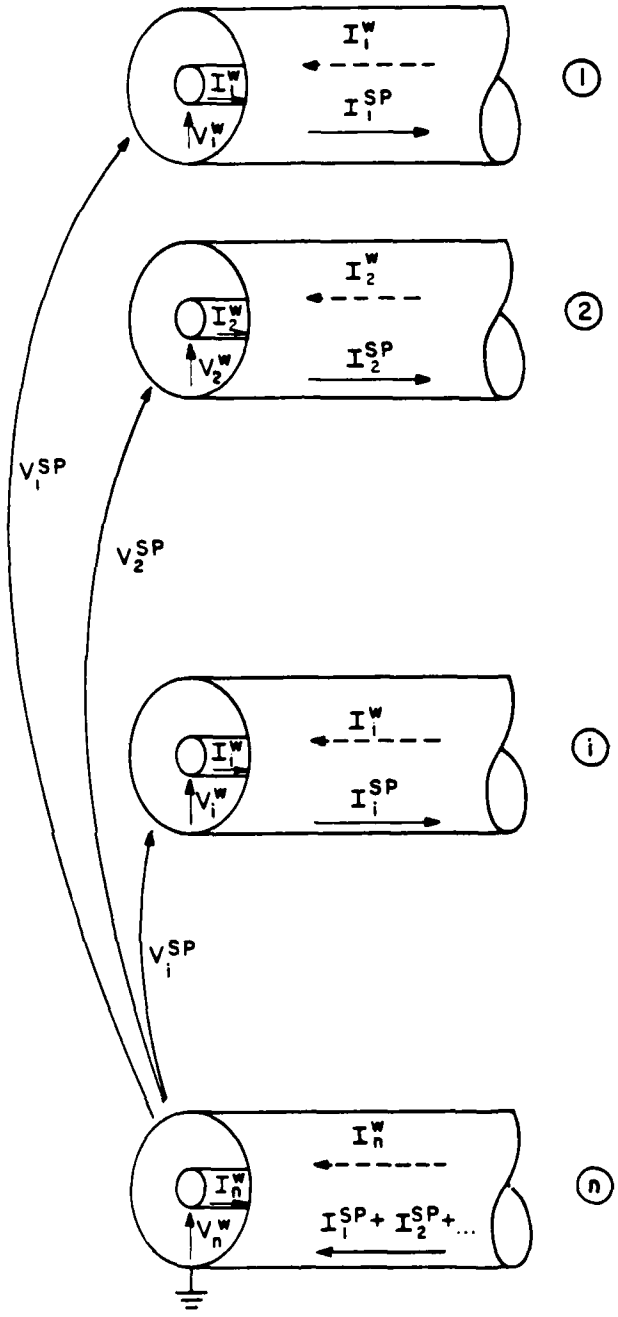

Figure 2.5 - Voltage and Current Definitions for the Shielded Section.

impedance, z_T, should be equal to the shield impedance, z_{SH}, up to the frequency at which the shield thickness is on the order of a skin depth.

The surface transfer impedance can be measured experimentally in a quadraxial test fixture [8,9,10] or calculated directly from the shield dimensions and characteristics [11]. Vance[11] states that the shield transfer impedance for solid shields can be calculated as

$$z_T = R_{DC}\left(\frac{\gamma d}{\sinh(\gamma d)}\right) \text{ ohms/meter} \qquad (2\text{-}15)$$

where R_{DC} is the per-unit-length D.C. resistance of the shield, d is the diameter of the shield, $\gamma = (1 + j)/\delta$ where $\delta = 1/\sqrt{\pi f \mu \sigma}$ is the skin depth of the shield, f is the frequency of operation, μ is the permeability of free space, and σ is the conductivity of the shield material. The formula in (2-15) assumes that the current is uniformly distributed around the periphery of the shield.

2.2 - MULTICONDUCTOR TRANSMISSION LINE MODEL FOR THE SHIELDED SECTION OF THE LINE

In this section, we wish to derive the multiconductor transmission line model for the shielded section of the flatpack, coaxial cable. The voltage and current definitions that are used in the derivation of the model are shown in Figure 2.5. The wire currents, I_i^W, are assumed to flow down the center conductor and return on the inside of

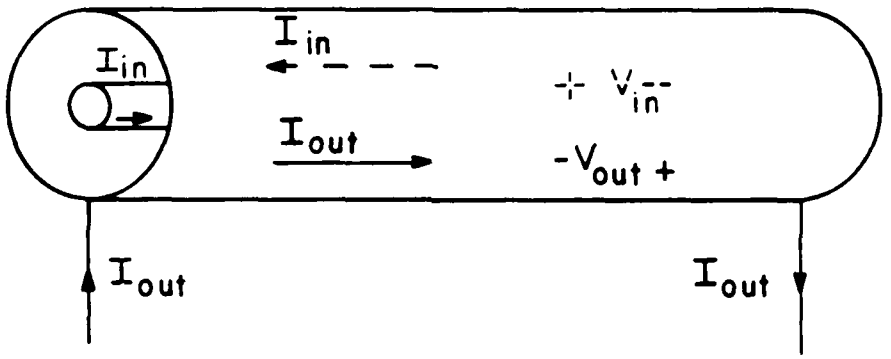

Figure 2.4 - Section of Coaxial Cable.

To illustrate the concept consider Figure 2.4 showing a coaxial cable. We assume that there are two distinct current paths in the circuit. First there is a current that flows on the outside of the shield and returns via a circuit external to the shield, this current is denoted I_{out}. The other current path consists of current flowing down the center conductor and returning on the inside of the shield and is denoted I_{in}. If a current I_{out} is flowing in the external circuit it will produce a per-unit-length voltage, V_{in}, along the inside of the shield via diffusion through the shield. This voltage will cause a current, I_{in}, to flow in the internal circuit. The converse is also true for a current flowing in the internal circuit. The surface transfer impedance, z_T, is then defined as

$$z_T = \frac{V_{in}}{I_{out}} \quad \text{ohms/meter} \tag{2-13a}$$

or equivalently

$$z_T = \frac{V_{out}}{I_{in}} \quad \text{ohms/meter} \tag{2-13b}$$

From this we can write an expression for the voltages on the inside and outside of the shield as

$$\begin{bmatrix} V_{in} \\ V_{out} \end{bmatrix} = \begin{bmatrix} z_{SH} & z_T \\ z_T & z_{SH} \end{bmatrix} \begin{bmatrix} I_{in} \\ I_{out} \end{bmatrix} \tag{2-14}$$

where z_{SH} denotes the impedance of the shield itself. It is worthwhile to note here that the surface transfer

conditions of the line into the equations.

This chapter will present all the background information and derivations needed to calculate the total chain parameter matrix for the flatpack, coaxial cable (with pigtail sections), incorporate the terminal conditions and to solve the equations uniquely for the voltages and currents at each end of the line. From these voltages and currents it will be possible to calculate the amount of electromagnetic crosstalk that will be present for a given line configuration.

2.1 - SHIELD TRANSFER IMPEDANCE

It is a well-known fact that if the shield of a coaxial cable were a perfect conductor there would be no coupling of electromagnetic fields present outside the shield to the inner conductor. If this were the case for the flatpack, coaxial cable then there would be no contribution to the total amount of crosstalk by the shielded section of the cable. The shields are not perfect conductors and therefore it is necessary to be able to describe the coupling of these electromagnetic fields over the shielded section. A fundamental concept which is used to explain this electromagnetic coupling to shielded wires is the surface transfer impedance. The concept was introduced by Schelkunoff in 1934 [5,6,7] and has been widely accepted.

and

$$\begin{bmatrix} \underline{V}_R \\ \underline{I}_R \end{bmatrix} = \begin{bmatrix} \quad \\ \underset{\sim}{\Phi}_{PR} \\ \quad \end{bmatrix} \begin{bmatrix} \underline{V}_{SR} \\ \underline{I}_{SR} \end{bmatrix} \tag{2-8}$$

Substituting equation (2-7) into equation (2-8) yields the result

$$\begin{bmatrix} \underline{V}_R \\ \underline{I}_R \end{bmatrix} = \begin{bmatrix} \quad \\ \underset{\sim}{\Phi}_{PR} \\ \quad \end{bmatrix} \begin{bmatrix} \quad \\ \underset{\sim}{\Phi}_{S} \\ \quad \end{bmatrix} \begin{bmatrix} \underline{V}_{SL} \\ \underline{I}_{SL} \end{bmatrix} \tag{2-9}$$

Substituting equation (2-6) into equation (2-9) gives the equation

$$\begin{bmatrix} \underline{V}_R \\ \underline{I}_R \end{bmatrix} = \begin{bmatrix} \quad \\ \underset{\sim}{\Phi}_{PR} \\ \quad \end{bmatrix} \begin{bmatrix} \quad \\ \underset{\sim}{\Phi}_{S} \\ \quad \end{bmatrix} \begin{bmatrix} \quad \\ \underset{\sim}{\Phi}_{PL} \\ \quad \end{bmatrix} \begin{bmatrix} \underline{V}_L \\ \underline{I}_L \end{bmatrix} \tag{2-10}$$

which relates the voltages and currents at the right end of the line to the voltages and currents at the left end of the line. We can then say that the total chain parameter matrix of the line, $\underset{\sim}{\Phi}_T$, is equal to the matrix product of all the chain parameter matrices of the individual sections taken in the proper order, i.e.,

$$\underset{\sim}{\Phi}_T = \underset{\sim}{\Phi}_{PR} \; \underset{\sim}{\Phi}_S \; \underset{\sim}{\Phi}_{PL} \tag{2-11}$$

for the case of our flatpack, coaxial cable.

Once the total chain parameter matrix, $\underset{\sim}{\Phi}_T$, is calculated we have an equation

$$\begin{bmatrix} \underline{V}_R \\ \underline{I}_R \end{bmatrix} = \begin{bmatrix} \quad \\ \underset{\sim}{\Phi}_{T} \\ \quad \end{bmatrix} \begin{bmatrix} \underline{V}_L \\ \underline{I}_L \end{bmatrix} \tag{2-12}$$

which only relates the voltages and currents at each end of the line. To solve explicitly for the terminal voltages and currents of the line we must incorporate the terminal

$$\underline{I}_{SR} = \begin{bmatrix} I_{SR1} \\ I_{SR2} \\ \vdots \\ I_{SR(2n-1)} \end{bmatrix} \qquad \underline{I}_{R} = \begin{bmatrix} I_{R1} \\ I_{R2} \\ \vdots \\ I_{R(2n-1)} \end{bmatrix}$$

The $\underset{\sim}{\Phi}_{PL}$ matrix is the chain parameter matrix of the left pigtail section and relates the voltages, $\underline{V}_{SL}$, and currents, $\underline{I}_{SL}$, at the left end of the shielded section to the voltages, $\underline{V}_{L}$, and currents, $\underline{I}_{L}$, at the left end of the line. The $\underset{\sim}{\Phi}_{S}$ matrix is the chain parameter matrix for the shielded section of the line and relates the voltages, $\underline{V}_{SR}$, and currents, $\underline{I}_{SR}$, at the right end of the shielded section to the voltages, $\underline{V}_{SL}$, and currents, $\underline{I}_{SL}$, at the left end of the shielded section. The $\underset{\sim}{\Phi}_{PR}$ matrix is the chain parameter matrix of the right pigtail section of the line and relates the voltages, $\underline{V}_{R}$, and currents, $\underline{I}_{R}$, at the right end of the line to the voltages, $\underline{V}_{SR}$, and currents, $\underline{I}_{SR}$, at the right end of the shielded section. We can relate the voltages and currents at each end of the three distinct sections as:

$$\begin{bmatrix} \underline{V}_{SL} \\ \underline{I}_{SL} \end{bmatrix} = \begin{bmatrix} \\ \underset{\sim}{\Phi}_{PL} \\ \\ \end{bmatrix} \begin{bmatrix} \underline{V}_{L} \\ \underline{I}_{L} \end{bmatrix} \qquad (2\text{-}6)$$

$$\begin{bmatrix} \underline{V}_{SR} \\ \underline{I}_{SR} \end{bmatrix} = \begin{bmatrix} \\ \underset{\sim}{\Phi}_{S} \\ \\ \end{bmatrix} \begin{bmatrix} \underline{V}_{SL} \\ \underline{I}_{SL} \end{bmatrix} \qquad (2\text{-}7)$$

be discussed later. As shown, the line can be broken into three distinct sections each having a uniform cross-section. It is possible to derive a chain parameter matrix for each of these sections individually and then, from these individual chain parameter matrices, obtain an overall chain parameter matrix for the whole line. To derive the overall chain parameter matrix we first show the voltage and current definitions at the end of each distinct section of the line with its corresponding chain parameter matrix as shown in Figure 2.3(b). The voltage and current vectors are defined as follows:

$$\underline{V}_L = \begin{bmatrix} V_{L1} \\ V_{L2} \\ \vdots \\ V_{L(2n-1)} \end{bmatrix} \quad \underline{V}_{SL} = \begin{bmatrix} V_{SL1} \\ V_{SL2} \\ \vdots \\ V_{SL(2n-1)} \end{bmatrix} \quad \underline{V}_{SR} = \begin{bmatrix} V_{SR1} \\ V_{SR2} \\ \vdots \\ V_{SR(2n-1)} \end{bmatrix}$$

$$\underline{V}_R = \begin{bmatrix} V_{R1} \\ V_{R2} \\ \vdots \\ V_{R(2n-1)} \end{bmatrix} \quad \underline{I}_L = \begin{bmatrix} I_{L1} \\ I_{L2} \\ \vdots \\ I_{L(2n-1)} \end{bmatrix} \quad \underline{I}_{SL} = \begin{bmatrix} I_{SL1} \\ I_{SL2} \\ \vdots \\ I_{SL(2n-1)} \end{bmatrix}$$

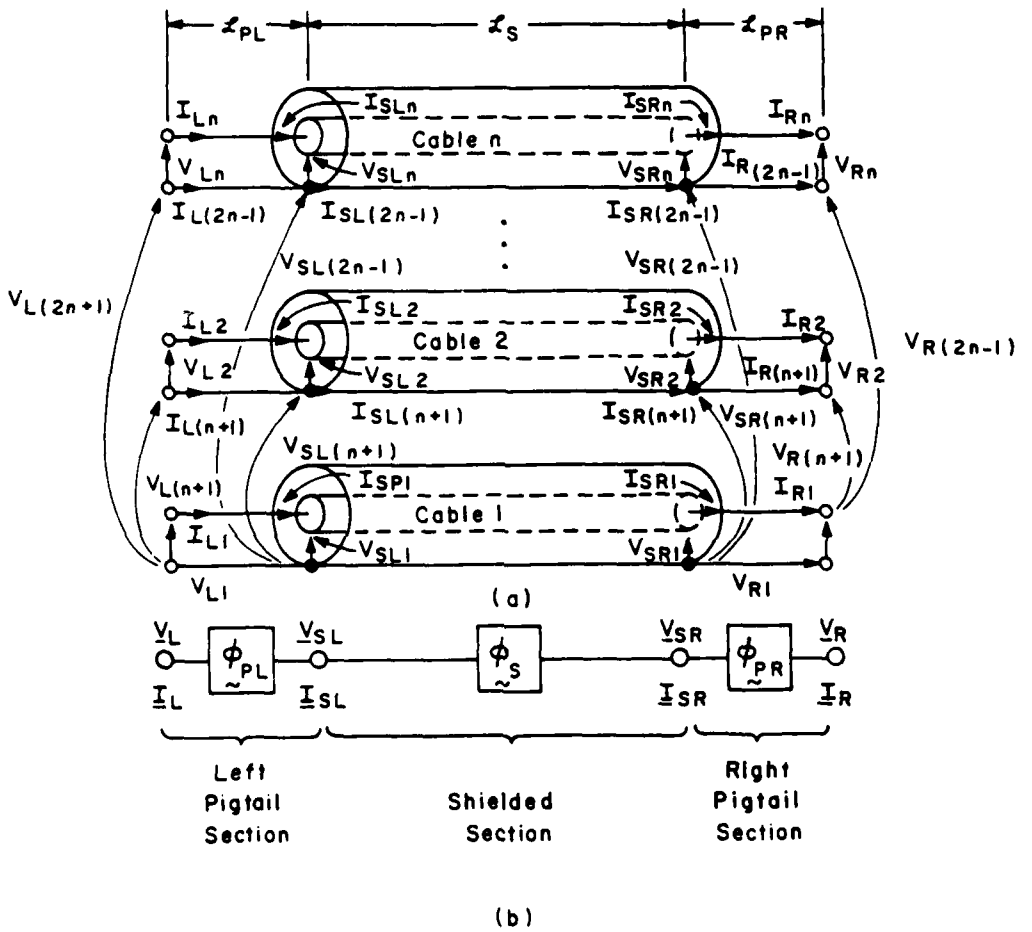

Figure 2.3 - Voltage and Current Definitions for the Flatpack, Coaxial Cable.

$$\frac{d\underline{I}(x)}{dx} = -\underset{\sim}{Y}\,\underline{V}(x) \qquad (2\text{-}4b)$$

where

$$\underline{V}(x) = \begin{bmatrix} V_1(x) \\ V_2(x) \\ \vdots \\ V_n(x) \end{bmatrix} \qquad \underline{I}(x) = \begin{bmatrix} I_1(x) \\ I_2(x) \\ \vdots \\ I_n(x) \end{bmatrix}$$

and the n x n matrices $\underset{\sim}{Z}$ and $\underset{\sim}{Y}$ are the per-unit-length impedance and admittance matrices, respectively.

The above MTL equations are a set of coupled, first order, ordinary differential equations which are quite similar to state-variable equations encountered in electric circuits and automatic controls[12]. Their solution is straightforward and of the form:

$$\begin{bmatrix} \underline{V}(\ell) \\ \underline{I}(\ell) \end{bmatrix} = \begin{bmatrix} \underline{\phi}(\ell) \end{bmatrix} \begin{bmatrix} \underline{V}(0) \\ \underline{I}(0) \end{bmatrix} \qquad (2\text{-}5)$$

where the line extends from x= 0 to x=ℓ. A comparison of (2-1) to (2-5) shows that the n+1 conductor transmission line is readily characterized as a 2n port via the chain parameter matrix representation discussed previously.

We will now adapt the above concepts to the characterization of flatpack, coaxial cables with exposed pigtail sections at each end as shown in Figure 2.3(a). The pigtails allow for connection to the individual wires and shields of each of the individual coaxial cables and will

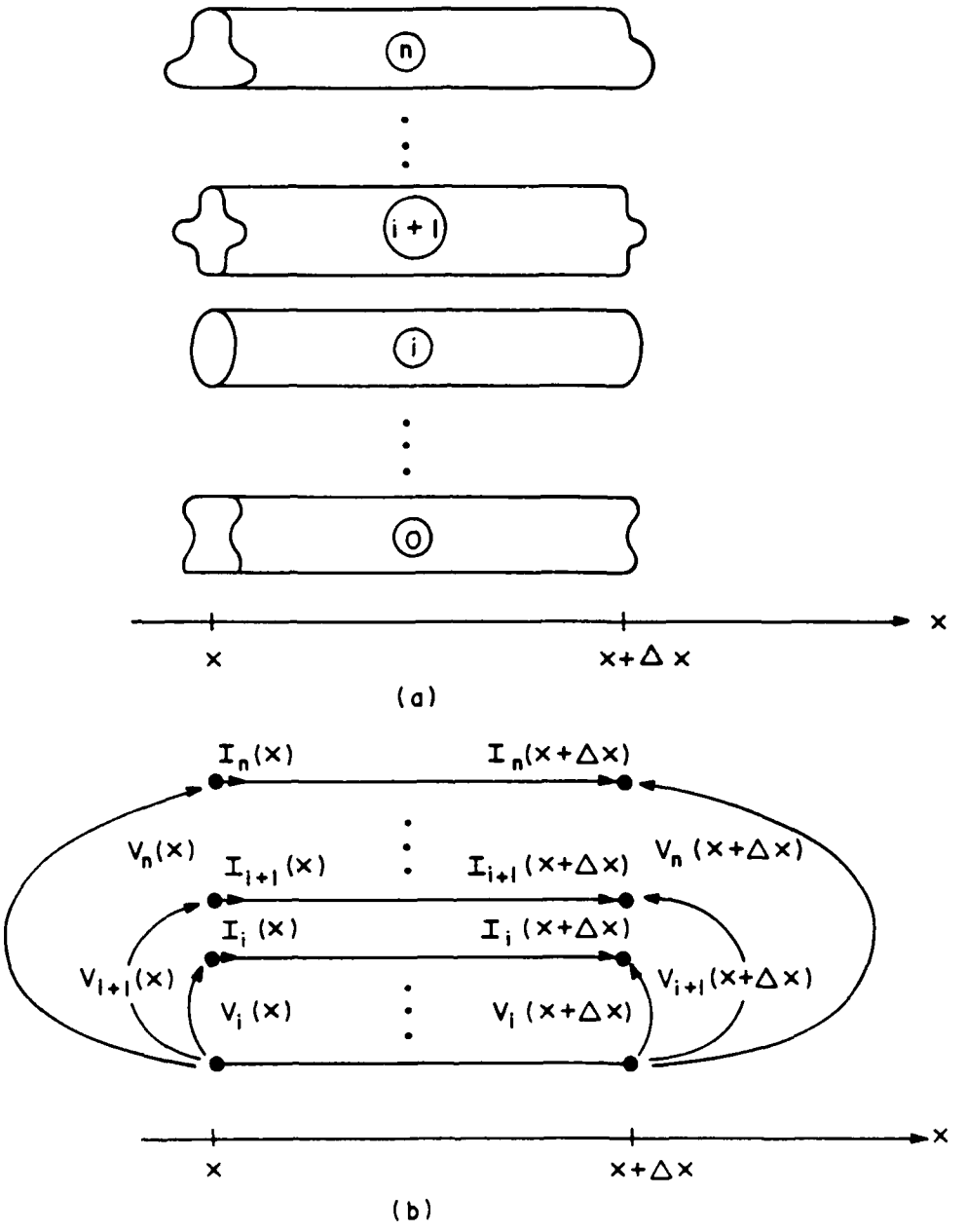

Figure 2.2 - General Transmission Line.

section (i=1,2,...,n). The equation is

$$\frac{\hat{V}_i^{sp}(R) - \hat{V}_i^{sp}(L)}{\Delta x} = -Z_{SH}\hat{I}_i^{sp} + Z_T\hat{I}_i^{w} - Z_{SH}\sum_{i=1}^{n-1}\hat{I}_i^{sp} - Z_T\hat{I}_n^{w} \quad (2\text{-}21)$$

Finally we must take in account the n^{th} wire, so we write the equation that relates the voltage of the n^{th} wire at the left end of the Δx section to the voltage of the n^{th} wire at the right end of the Δx section, which is

$$\frac{\hat{V}_n^{w}(R) - \hat{V}_n^{w}(L)}{\Delta x} = -Z_{con}\hat{I}_n^{w} - Z_{SH}\hat{I}_n^{w} - Z_T\sum_{i=1}^{n-1}\hat{I}_i^{sp} \quad (2\text{-}22)$$

Combining equations (2-20), (2-21), and (2-22) into a matrix form and taking the limit as $\Delta x \to 0$ we can then write the per-unit-length impedance matrix for the shielded section of the cable, $\underset{\sim}{Z}_C$, as

$$-\begin{bmatrix} \hat{V}_1^{w} \\ \hat{V}_2^{w} \\ \vdots \\ \hat{V}_n^{w} \\ -- \\ \hat{V}_1^{sp} \\ \hat{V}_2^{sp} \\ \vdots \\ \hat{V}_{n-1}^{sp} \end{bmatrix} = \underset{\sim}{Z}_C \underline{I} = \left[\begin{array}{cccc|ccccc} Z_{con}+Z_{SH} & & & & -Z_T & & & & \\ & \ddots & & \varnothing & & \ddots & & \varnothing & \\ & & Z_{con}+Z_{SH} & & & & -Z_T & & \\ & \varnothing & & & & \varnothing & & & -Z_T \\ \hline Z_T & Z_T & \cdots & Z_T & & & & & \\ \hline -Z_T & & & Z_T & 2Z_{SH} & & & & \\ & \ddots & & \vdots & & \ddots & & \varnothing & \\ & & -Z_T & Z_T & & & Z_{SH} & & \\ & \varnothing & & & & Z_{SH} & & 2Z_{SH} & \\ & & & & & & 2Z_{SH} & & \end{array}\right] \begin{bmatrix} I_1^{w} \\ I_2^{w} \\ \vdots \\ I_n^{w} \\ I_1^{sp} \\ I_2^{sp} \\ \vdots \\ I_{n-1}^{sp} \end{bmatrix} \quad (2\text{-}23)$$

where $\dot{V}_i$ is the derivative of V_i with respect to x.

Next we will derive the per-unit-length inductance matrix of the shielded section, $\underset{\sim}{L}_S$. We can divide the inductance matrix into four distinct parts

$$\underset{\sim}{L}_S = \left[\begin{array}{c|c} \underset{\sim}{L}^{ww} & \underset{\sim}{L}^{spw} \\ \hline \underset{\sim}{L}^{wsp} & \underset{\sim}{L}^{spsp} \end{array}\right] \tag{2-24}$$

which implies

$$\underline{\Psi}_w = \underset{\sim}{L}^{ww}\,\underline{I}^w + \underset{\sim}{L}^{spw}\,\underline{I}^{sp} \tag{2-25a}$$

and

$$\underline{\Psi}_s = \underset{\sim}{L}^{wsp}\,\underline{I}^w + \underset{\sim}{L}^{spsp}\,\underline{I}^{sp} \tag{2-25b}$$

$$\underline{\Psi}_w = \begin{bmatrix} \Psi_w^1 \\ \Psi_w^2 \\ \vdots \\ \Psi_w^n \end{bmatrix}$$

where Ψ_w^i is the flux penetrating the i^{th} wire circuit and

$$\underline{\Psi}_S = \begin{bmatrix} \Psi_S^1 \\ \Psi_S^2 \\ \vdots \\ \Psi_S^{n-1} \end{bmatrix}$$

where Ψ_S^i is the flux penetrating the i^{th} shield circuit.

Each entry in the L_S matrix, l_{ij}, can be calculated directly by using the formula

$$l_{ij} = \frac{\Psi_i}{I_j} \text{ henrys/meter} \tag{2-26}$$

which states that the inductance between the i^{th} and j^{th}

circuit can be calculated as the flux that penetrates the i^{th} circuit, Ψ_i, due to a current flowing in the j^{th} circuit, I_j.

First we will calculate the entries of the $\underset{\sim}{L}^{ww}$ submatrix of $\underset{\sim}{L}_S$ which relates the currents flowing in the n wire circuits to the flux penetrating each of the n wire circuits. This can be accomplished by evaluating equation (2-25a) with all the shield currents being set to zero, i.e., $\underline{I}^{sp} = \underline{0}$. For this submatrix of the $\underset{\sim}{L}_S$ matrix each entry l_{ij} refers to the flux penetrating the i^{th} wire circuit, Ψ_i, due to a current, I_j, flowing in the j^{th} wire circuit with all other currents set to zero.

We will first calculate the diagonal terms of this submatrix or l_{ii} for i = 1,2,...,n. In other words we need to calculate the flux penetrating the i^{th} wire circuit, Ψ_i, due to a current flowing in that i^{th} wire circuit, I_i. With all other currents set to zero we are simply trying to calculate the inductance of a single coaxial cable. Referring to Figure 2.7 we can calculate this inductance as

$$l = \frac{\mu_o}{2\pi} \ln\left(\frac{R_{shd}}{R_{wc}}\right) \qquad (2\text{-}27)$$

where R_{shd} is the radius of the shield and R_{wc} is the radius of the center conductor.

Next we consider the off-diagonal terms of the $\underset{\sim}{L}^{ww}$ submatrix, i.e., l_{ij} for $i \neq j$. Consider Figure 2.8 where

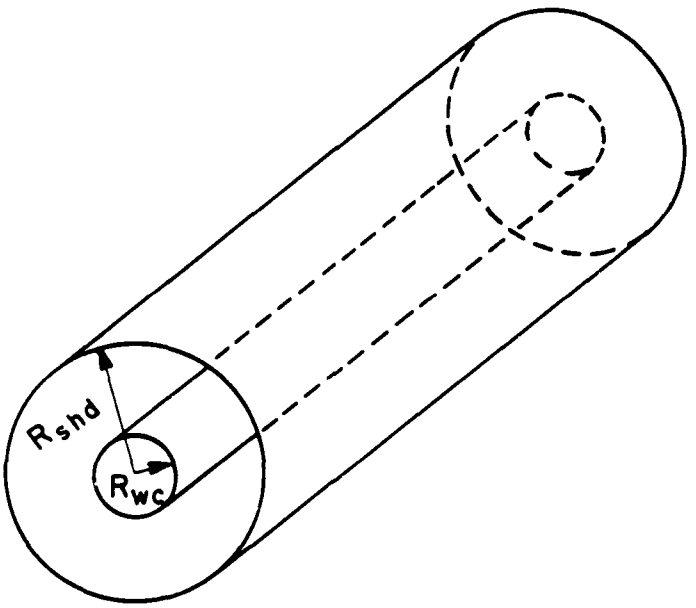

Figure 2.7 - Cross-Section of the Shielded Section of the Cable.

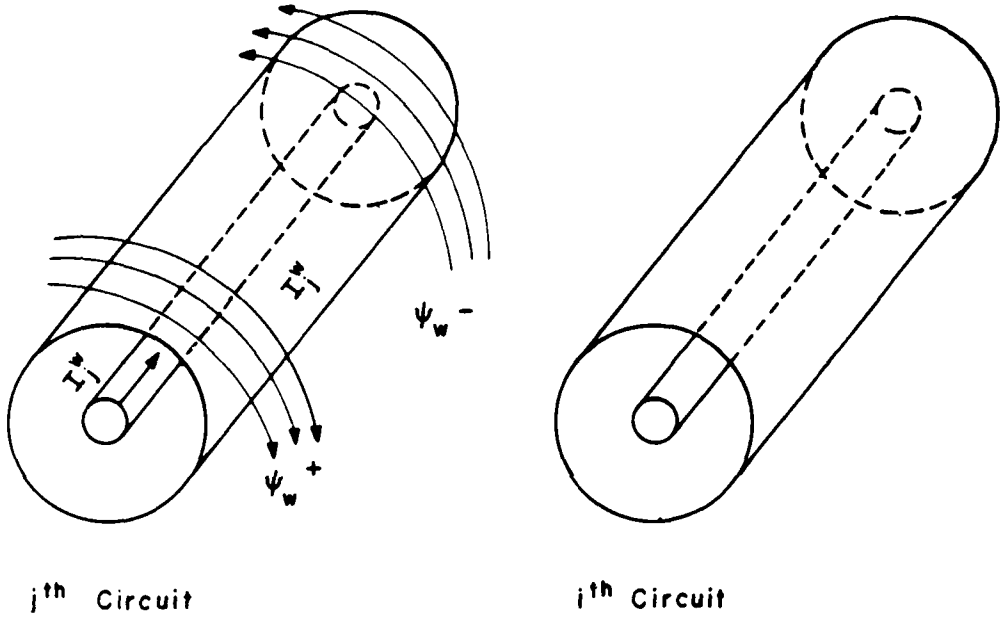

Figure 2.8 - Flux Generated by the j^{th} Shield Circuit.

we consider the flux generated by the j^{th} wire circuit. The current, I_j^w, flowing down the center conductor generates a flux, ψ_w^+, in the direction indicated. This current returns via the interior of the j^{th} shield and generates a flux, ψ_w^-, as shown in Figure 2.8. The two fluxes generated, ψ_w^+ and ψ_w^-, are of equal magnitude but opposite in direction therefore they cancel each other in the region exterior to the shield. This cancellation implies that there will be no net flux present outside the j^{th} wire circuit and linking the i^{th} wire circuit therefore $[l_{ij}]_{i\neq j}=0$ for the $\underset{\sim}{L}^{ww}$ submatrix. From this we can state that

$$\underset{\sim}{L}^{ww} = \begin{bmatrix} l_{11} & & & \\ & l_{22} & & \emptyset \\ & & \ddots & \\ \emptyset & & & l_{nn} \end{bmatrix} \qquad (2\text{-}28)$$

where l_{ii} is the quantity stated in (2-27).

Next we will calculate the $\underset{\sim}{L}^{wsp}$ submatrix of $\underset{\sim}{L}_S$ which relates the currents flowing in the n wire circuits to the flux penetrating each of the n-1 shield circuits. This can be accomplished by solving equation (2-25b) with all the shield currents set to zero, i.e., $\underline{I}^{sp}=\underline{0}$. Each term, l_{ij}, in the $\underset{\sim}{L}^{wsp}$ submatrix relates the flux, ψ_i, penetrating the i^{th} shield circuit due to a current, I_j, flowing in the j^{th} wire circuit. This configuration is shown in Figure 2.9. As before we have two fluxes, ψ_w^+ and ψ_w^-, that are present outside the j^{th} wire circuit due to current flowing down the center conductor and returning on the interior of the

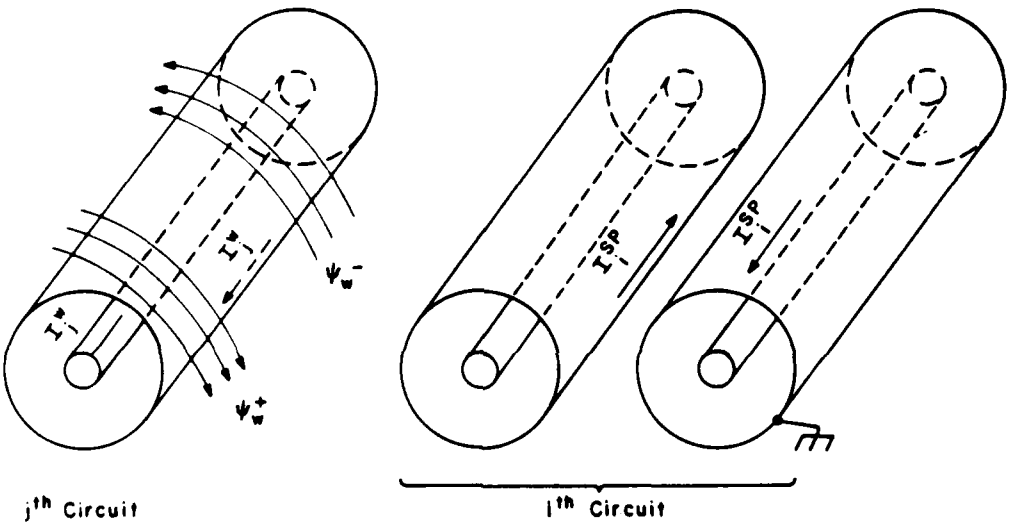

Figure 2.9 - Flux Penetrating the i^{th} Shield Circuit.

shield. Again these two fluxes are equal in magnitude but opposite in direction therefore the net flux present outside the j^{th} wire circuit is equal to zero. Since there is no flux present outside the j^{th} wire circuit that can penetrate and link the i^{th} shield circuit, all the entries in the $\underset{\sim}{L}^{wsp}$ submatrix will be zero. In matrix form we can state

$$\underset{\sim}{L}^{wsp} = \underset{\sim}{0} \tag{2-29}$$

Next we consider the $\underset{\sim}{L}^{spw}$ submatrix of $\underset{\sim}{L}_S$ which relates the currents flowing in the n-1 shield circuits due to the flux penetrating each of the n wire circuits due to this current. This could be calculated by solving equation (2-25a) with all the wire currents set to zero, i.e., $\underline{I}^w=\underline{0}$. Instead of calculating these entries in the submatrix it can be argued that since the medium surrounding the line is reciprocal, the $\underset{\sim}{L}_S$, $\underset{\sim}{Z}_S$, and $\underset{\sim}{C}_S$ matrices for the line must be symmetric. For the $\underset{\sim}{L}_S$ matrix to be symmetric $\underset{\sim}{L}^{spw}$ must equal $(\underset{\sim}{L}^{wsp})^t$ (t represents the matrix transpose), so for our situation

$$\underset{\sim}{L}^{spw} = \underset{\sim}{0}^t = \underset{\sim}{0} \tag{2-30}$$

Finally we must calculate the $\underset{\sim}{L}^{spsp}$ submatrix of $\underset{\sim}{L}_S$ which relates the currents flowing in the n-1 shield circuits to the flux penetrating the n-1 shield circuits. Each entry, l_{ij}, in the $\underset{\sim}{L}^{spsp}$ submatrix relates the flux, Ψ_i, penetrating the i^{th} shield circuit due to a current,

I_j, flowing in the j^{th} shield circuit. It is possible to calculate these entries by solving equation (2-25b) with all the wire currents set to zero, i.e., $\underline{I}^W = \underline{0}$. To calculate these entries consider Figure 2.10 showing the dimensioned cross section of the flatpack, coaxial cable where WS is the center-to-center wire separation of adjacent coaxes, R_{shd} is the interior radius of the shields, and t_s is the thickness of each of the shields.

Since all the currents are flowing down and returning on the exterior of the shields we can consider the flatpack, coaxial cable as n "fat wires" for the computation of $\underset{\sim}{L}^{spsp}$. These n "fat wires" will each have a radius of $R_{shd} + t_s$ and the n^{th} conductor will be grounded. The entries, l_{ij}, in the $\underset{\sim}{L}^{spsp}$ submatrix can be calculated by calculating the inductance matrix of these n "fat wires" directly from the formulas [12]

$$l_{ii} = \frac{\mu_o}{2\pi} \ln \left(\frac{d_{io}^2}{r_{wi}\, r_{wo}} \right) \qquad (2\text{-}30a)$$

$$l_{ij} = \frac{\mu_o}{2\pi} \ln \left(\frac{d_{io}\, d_{jo}}{r_{wo}\, d_{ij}} \right) \quad \text{for } i \neq j \qquad (2\text{-}30b)$$

where d_{io} represents the distance between the i^{th} conductor and the reference conductor, d_{jo} represents the distance between the j^{th} conductor and the reference conductor, d_{ij} is the distance between the i^{th} and j^{th} conductors, r_{wi} is the radius of the i^{th} wire, and r_{wo} is the radius of the

reference conductor. The distance d_{io} can be calculated as $d_{io} = (n-i) \times WS$. The distance d_{jo} can similarly be calculated as $d_{jo} = (n - j) \times WS$. The distance d_{ij} can be calculated as $d_{ij} = |i - j| \times WS$. And as stated previously the radius of each of the "fat wires" and the reference conductor is $R_{shd} + t_s$. Combining these we obtain

$$l_{ii} = \frac{\mu_o}{2\pi} \ln \left[\frac{((n - i) \times WS)^2}{(R_{shd} + t_s)^2} \right]$$

which reduces to

$$l_{ii} = \frac{\mu_o}{\pi} \ln \left[\frac{(n - i) \times WS}{R_{shd} + t_s} \right] \qquad (2\text{-}31a)$$

and for the off-diagonal terms we obtain

$$l_{ij} = \frac{\mu_o}{2\pi} \ln \left[\frac{[(n - i) \times WS][(n - j) \times WS]}{[|i - j| \times WS]\ (R_{shd} + t_s)} \right]$$

which reduces to

$$l_{ij} = \frac{\mu_o}{2\pi} \ln \left[\frac{(n - i)(n - j) \times WS}{|i - j|\ (R_{shd} + t_s)} \right] \text{ for } i \neq j \qquad (2\text{-}31b)$$

Next we turn our attention to deriving the per-unit-length capacitance matrix of the shielded section, $\underset{\sim}{C}_S$. As with the L_S matrix, we can divide the $\underset{\sim}{C}_S$ matrix into four distinct parts

$$\underset{\sim}{C}_S = \left[\begin{array}{c|c} \underset{\sim}{C}^{ww} & \underset{\sim}{C}^{spw} \\ \hline \underset{\sim}{C}^{wsp} & \underset{\sim}{C}^{spsp} \end{array} \right] \qquad (2\text{-}32)$$

which implies

$$\underline{q}_w = \underset{\sim}{C}^{ww}\,\underline{V}^w + \underset{\sim}{C}^{spw}\,\underline{V}^{sp} \qquad (2\text{-}33a)$$

and

$$\underline{q}_S = \underset{\sim}{C}^{wsp}\,\underline{V}^w + \underset{\sim}{C}^{spsp}\,\underline{V}^{sp} \qquad (2\text{-}33b)$$

$$\underline{q}_w = \begin{bmatrix} 1 \\ q_w \\ q_w^2 \\ \cdot \\ \cdot \\ \cdot \\ n \\ q_w \end{bmatrix}$$

where q_w^i is the charge present on the i^{th} wire circuit and

$$\underline{q}_S = \begin{bmatrix} 1 \\ q_S \\ q_S^2 \\ \cdot \\ \cdot \\ \cdot \\ q_S^{n-1} \end{bmatrix}$$

where q_S^i is the charge present on the i^{th} shield circuit.

First we will calculate the $\underset{\sim}{C}^{ww}$ submatrix of $\underset{\sim}{C}_S$ which relates the voltages of the n wires to the charges present on the n wires when all the shield voltages are set to zero, i.e., $\underline{V}^{sp} = \underline{0}$. We will first calculate the diagonal terms, c_{ii} for i=1,2,...,n, for this submatrix. In other words we need to calculate the charge present on the i^{th} wire circuit due to a voltage on the i^{th} wire circuit. With all other voltages set to zero we are simply trying to calculate the capacitance of a single coaxial cable.

Referring to Figure 2.7 we can calculate this capacitance as

$$c_{ii} = \frac{2\pi\varepsilon}{\ln\left(\frac{R_{shd}}{R_{wc}}\right)} \qquad (2\text{-}34)$$

where R_{shd} is the radius of the shield , R_{wc} is the radius of the center conductor, and ε is the permittivity of the insulation interior to each shield.

Next we consider the off-diagonal terms of the $\underset{\sim}{C}^{ww}$ submatrix, i.e., c_{ij} for $i \neq j$. We can represent all the capacitances present in the shielded section of the flat-pack, coaxial cable by the equivalent circuit shown in Figure 2.11. The capacitances present inside the coaxial cables are the c_{ii} terms of the $\underset{\sim}{C}^{ww}$ submatrix that we previously calculated. The c_{ij} terms we are now trying to calculate are the charges present on the i^{th} wire circuit due to a voltage of the j^{th} wire circuit which would be represented by a capacitance from the i^{th} center conductor to the j^{th} center conductor. Due to the electostatic shielding by the coaxial shields there will be no capacitance between these conductors as shown in Figure 2.11 therefore we can state that

$$[c_{ij}]_{i\neq j} = 0 \qquad (2\text{-}35)$$

Combining (2-34) and (2-35) into matrix form we can state that the C^{ww} be represented as shown in equation (2-36).

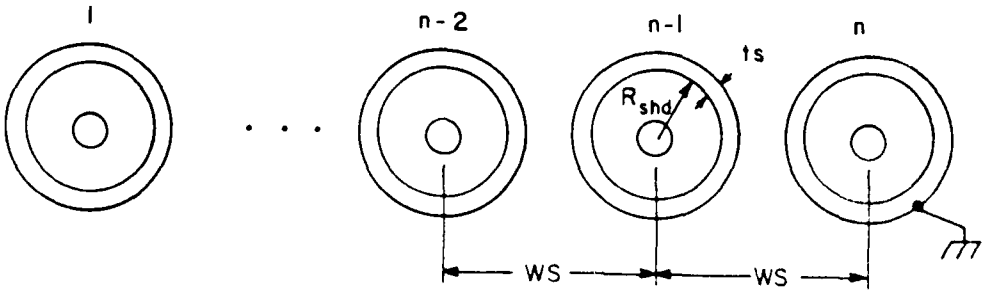

Figure 2.10 - Cross-Section of the Flatpack, Coaxial Cable.

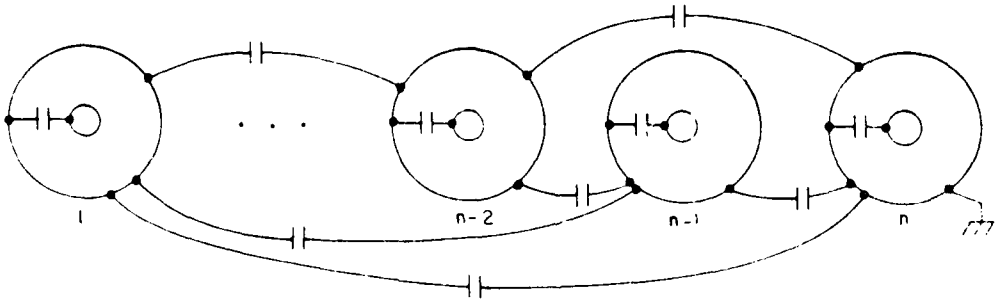

Figure 2.11 - Equivalent Circuit for the Capacitances of the Shielded Section.

$$\underset{\sim}{C}^{ww} = \begin{bmatrix} c_{11} & & & \\ & c_{22} & & \\ & & \ddots & \\ & & & c_{nn} \end{bmatrix} \quad \text{(2-36)}$$

Next we consider the $\underset{\sim}{C}^{wsp}$ submatrix of $\underset{\sim}{C}_S$ which relates the charges present on the n-1 shield circuits due to the voltages of the n wire circuits. This can be accomplished by solving (2-33b) with all the shield voltages set to zero, i.e., $\underline{V}^{sp} = \underline{0}$. But, as before due to electrostatic shielding the voltages inside the coaxial cables will produce no charges outside these cables therefore we can state that

$$\underset{\sim}{C}^{wsp} = [\underset{\sim}{0}] \quad \text{(2-37)}$$

Next we must calculate the $\underset{\sim}{C}^{spw}$ submatrix of $\underset{\sim}{C}_S$ which relates the charges present on the n wire circuits to the voltages of the n-1 shield circuits. This submatrix could be calculated by solving equation (2-33a) with all the wire voltages set to zero, i.e., $\underline{V}^{w} = \underline{0}$. As before with the case of the inductance matrix we can argue that the $\underset{\sim}{C}_S$ matrix must be symmetric since the surrounding medium is reciprocal. For the $\underset{\sim}{C}_S$ matrix to be symmetric $\underset{\sim}{C}^{spw}$ must equal $(\underset{\sim}{C}^{wsp})^t$ therefore we can state that

$$\underset{\sim}{C}^{spw} = \underset{\sim}{0}^t = \underset{\sim}{0} \quad \text{(2-38)}$$

Finally we must calculate the $\underset{\sim}{C}^{spsp}$ submatrix of $\underset{\sim}{C}_S$ which relates the charges present on the n-1 shield circuits to the voltages of the n-1 shield circuits. To calculate this submatrix we can again model the flatpack,

is shown in Figure 2.17. There are two contributions to the net inductance for this situation. The first, l_1, is due to the current flowing down the i^{th} shield pigtail and can be calculated as

$$l_1 = -\frac{\mu_o}{2\pi} \ln\left(\frac{d_3}{R_{pd}}\right) \tag{2-54}$$

The second contribution, l_2, is due to the current returning on the n^{th} shield pigtail and can be calculated as

$$l_2 = -\frac{\mu_o}{2\pi} \ln\left(\frac{d_1}{d_2}\right) \tag{2-55}$$

The three distances needed to solve equations (2-54) and (2-55) can be calculated as

$$d_1 = \sqrt{[(n - i) \times WS + s]^2 + d^2}$$

$$d_2 = (n - i) \times WS$$

$$d_3 = \sqrt{d^2 + s^2}$$

Substituting these distances into equations (2-54) and (2-55) and summing them to get the total inductance yields

$$l_{ii} = -\frac{\mu_o}{2\pi} \ln\left[\frac{\sqrt{s^2 + d^2}}{R_{pd}}\right] + \frac{\mu_o}{2\pi} \ln\left[\frac{\sqrt{[(n-i)xWS + s]^2 + d^2}}{(n - i) \times WS}\right]$$

which reduces to

$$l_{ii} = \frac{\mu_o}{2\pi} \ln\left[\frac{R_{pd}\ \sqrt{[(n - i) \times WS + s]^2 + d^2}}{\sqrt{s^2 + d^2} \times (n - i) \times WS}\right] \tag{2-56}$$

Next we will calculate the terms of the L^{wsp} that lie in region 1 of (2-53). For this region of the submatrix $j>i$ and its corresponding representation is shown in Figure (2.18). Again there are two contributions to the net

inductance

$$l_{ij} = -\frac{\mu_o}{2\pi} \ln\left[\frac{(j - i) \times WS}{R_{pd}}\right] + \frac{\mu_o}{2\pi} \ln\left[\frac{(n - j) \times WS}{R_{pd}}\right] + \frac{\mu_o}{2\pi} \ln\left[\frac{(n - i) \times WS}{R_{pd}}\right]$$

which reduces to

$$l_{ij} = \frac{\mu_o}{2\pi} \ln\left[\frac{(n - j)(n - i) \times WS}{(j - i) \times R_{pd}}\right] \qquad (2\text{-}51)$$

The equation in (2-51) was derived for the case $j > i$ but since the per-unit-length parameter matrices must be symmetric, this equation can be extended to the general case by modifying the equation to become

$$l_{ij} = \frac{\mu_o}{2\pi} \ln\left[\frac{(n - j)(n - i) \times WS}{|j - i| \times R_{pd}}\right] \qquad (2\text{-}52)$$

Next we will calculate the $\underset{\sim}{L}^{wsp}$ submatrix of $\underset{\sim}{L}_p$ which relates the flux penetrating and linking the n wire circuits to the currents flowing in the n-1 shield circuits. The $\underset{\sim}{L}^{wsp}$ is rectangular and looks as follows

$$\underset{\sim}{L}^{wsp} = \left[\begin{array}{c|c} \text{region 1} & \\ & \text{region 3} \\ \text{region 2} & \end{array}\right] \qquad (2\text{-}53)$$

We will start by calculating the elements that are on the principal diagonal of this submatrix, whose representation

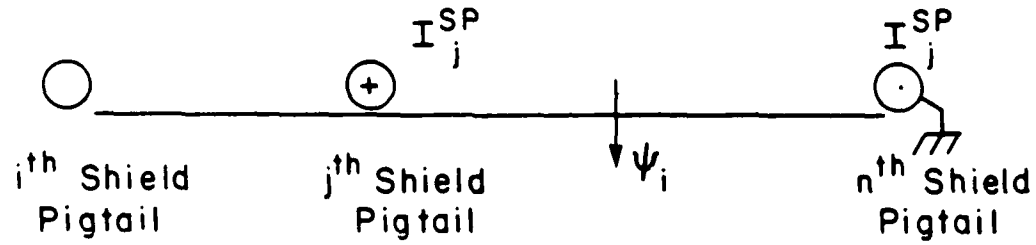

Figure 2.16 - Mutual Inductance of the i^{th} and j^{th} Shield Circuits over the Pigtail Sections.

yields

$$l_{ii} = \frac{\mu_o}{2\pi} \ln\left[\frac{[(n - i) \times WS]^2}{R_{pd}^2}\right]$$

which reduces to

$$l_{ii} = \frac{\mu_o}{\pi} \ln\left[\frac{(n - i) \times WS}{R_{pd}}\right] \qquad (2\text{-}50)$$

Now we will calculate the off-diagonal terms of the $\underset{\sim}{L}^{spsp}$ submatrix of L_p. This situation is shown in Figure 2.16 for $j > i$. The total inductance can be thought of as having three contributions, the first, l_1, is due to the flux penetrating the i^{th} shield circuit to the left of the j^{th} shield pigtail due to the current flowing down the j^{th} shield pigtail. The second, l_2, is due to the flux penetrating the i^{th} shield circuit to the right of the the j^{th} shield pigtail due to the current flowing down the j^{th} shield pigtail. The third, l_3, is due to the flux penetrating the i^{th} shield circuit due to the current returning on the reference conductor (the n^{th} shield pigtail). We can calculate each of these contributions as follows

$$l_1 = -\frac{\mu_o}{2\pi} \ln\left[\frac{(j - i) \times WS}{R_{pd}}\right]$$

$$l_2 = \frac{\mu_o}{2\pi} \ln\left[\frac{(n - j) \times WS}{R_{pd}}\right]$$

$$l_3 = \frac{\mu_o}{2\pi} \ln\left[\frac{(n - i) \times WS}{R_{pd}}\right]$$

Summing these three contributions gives us the total

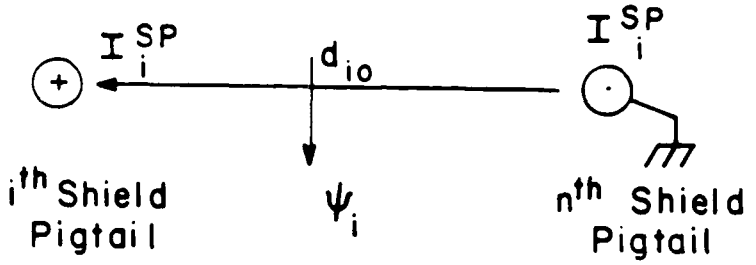

Figure 2.15 - Self Inductance of the i^{th} Shield Circuit over the Pigtail Sections.

yields

$$l_{ij} = -\frac{\mu_o}{2\pi} \ln\left[\frac{(j - i) \times WS}{\sqrt{[((j - i) \times WS) - s]^2 + d^2}}\right] + \frac{\mu_o}{2} \ln\left[\frac{\sqrt{[((j - i) \times WS) + s]^2 + d^2}}{(j - i) \times WS}\right]$$

which reduces to

$$l_{ij} = \frac{\mu_o}{2\pi} \ln\left[\frac{\sqrt{[(j-i)xWS-s]^2 + d^2}\sqrt{[(j-i)xWS+s]^2 + d^2}}{[(j-i)xWS]^2}\right] \quad (2\text{-}48)$$

The equation given in (2-48) was derived for the case $j > i$, but since the per-unit-length parameter matrices must be symmetric as stated earlier we can modify (2-48) to handle all l_{ij} entries for $i \neq j$. This equation will then become

$$l_{\substack{ij \\ i\neq j}} = \frac{\mu_o}{2\pi} \ln\left[\frac{\sqrt{[|j-i|xWS-s]^2 + d^2}\sqrt{[|j-i|xWS+s]^2 + d^2}}{[|j-i|xWS]^2}\right] \quad (2\text{-}49)$$

We have now derived equations (2-45) and (2-49) which specify all entries in the $\underset{\sim}{L}^{ww}$ submatrix of $\underset{\sim}{L}_P$.

Next we calculate the L^{spsp} submatrix of $\underset{\sim}{L}_P$ which relates the flux penetrating and linking the n-1 shield circuits to the currents flowing in those n-1 shield circuits. We will first consider the main diagonal terms of this submatrix which are the self inductances of each of the n-1 shield circuits. This situation is shown in Figure 2.15, where d_{io} can be calculated as $d_{io} = (n-i) \times WS$. Substituting d_{io} and the wire radius in equation (2-30a)

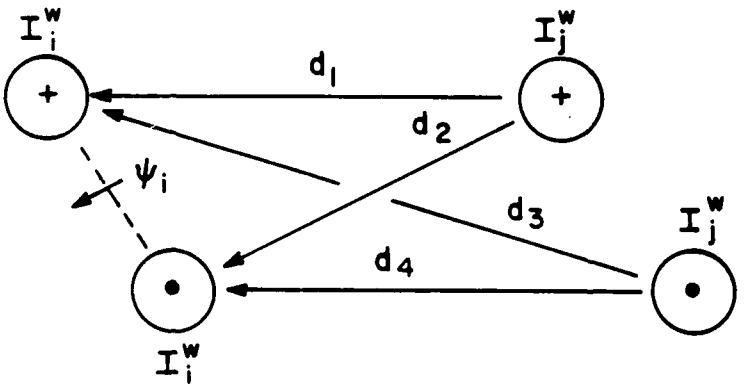

Figure 2.14 - Mutual Inductance of the i^{th} and j^{th} Wire Circuits over the Shielded Section.

Now we will calculate the off-diagonal terms of the $\underset{\sim}{L}^{ww}$ submatrix of $\underset{\sim}{L}_p$. This case is shown for the i^{th} and j^{th} wire circuits in Figure 2.14 for $j > i$. To calculate these inductances we will need to consider the flux penetrating the i^{th} wire circuit due to the current flowing down the j^{th} center conductor plus the flux penetrating the i^{th} wire circuit due to that same current returning on the j^{th} shield pigtail. The contribution to the total inductance by the current flowing down the j^{th} center conductor can be calculated as

$$l_1 = - \frac{\mu_o}{2\pi} \ln\left(\frac{d_1}{d_2}\right) \text{ henrys/meter} \qquad (2\text{-}46)$$

The contribution made by the current returning on the j^{th} shield can be calculated as

$$l_2 = - \frac{\mu_o}{2\pi} \ln\left(\frac{d_3}{d_4}\right) \text{ henrys/meter} \qquad (2\text{-}47)$$

Using the dimensions given in Figure 2.12(b) it is possible to calculate the needed distances as

$$d_1 = (j - i) \times WS$$

$$d_2 = \sqrt{[((j - i) \times WS) - s)]^2 + d^2}$$

$$d_3 = \sqrt{[((j - i) \times WS) + s)]^2 + d^2}$$

$$d_4 = (j - i) \times WS$$

The total inductance l_{ij} is equal to the sum of the individual contributions l_1 and l_2. Substituting these distances into equation (2-46) and (2-47) and taking their sum

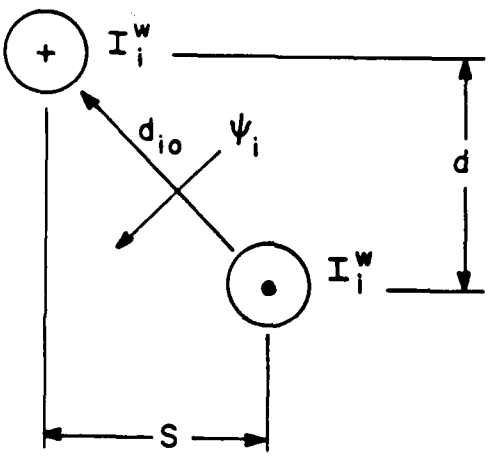

Figure 2.13 - Self Inductance of the i^{th} Wire Circuit over the Pigtail Sections.

the center conductors and the conductors connected to the shields) are perfect conductors. This assumption will make $\underset{\sim}{Z}_{CP} = \underset{\sim}{0}$ for the pigtail sections leaving only the $\underset{\sim}{L}_P$ and $\underset{\sim}{C}_P$ matrices to be calculated.

First we will derive the per-unit-length inductance matrix, $\underset{\sim}{L}_P$, for the representation shown in Figure 2.12(b). As in the previous section we will divide the inductance matrix into four distinct parts

$$\underset{\sim}{L}_P = \left[\begin{array}{c|c} \underset{\sim}{L}^{ww} & \underset{\sim}{L}^{spw} \\ \hline \underset{\sim}{L}^{wsp} & \underset{\sim}{L}^{spsp} \end{array}\right] \qquad (2\text{-}44)$$

which implies the same equations stated in (2-25a) and (2-25b). Each entry in the $\underset{\sim}{L}_P$ matrix, l_{ij}, can be calculated directly using the equations presented in (2-30a) and (2-30b).

First we will calculate the $\underset{\sim}{L}^{ww}$ submatrix of $\underset{\sim}{L}_P$ which relates the flux penetrating and linking the n wire circuits to the currents flowing in these n wire circuits. We will first consider the diagonal terms of this submatrix which are the self inductances of each of the n wire circuits. The case we need to consider for the i^{th} circuit is shown in Figure 2.13. From this figure we can see that $d_{ic} = \sqrt{s^2 + d^2}$. Substituting this and the wire radius into equation (2-30a) yields l_{ii} for the $\underset{\sim}{L}^{ww}$ submatrix as

$$l_{ii} = \frac{\mu_o}{2\pi} \ln\left[\frac{s^2 + d^2}{R_{pc}\, R_{pd}}\right] \qquad (2\text{-}45)$$

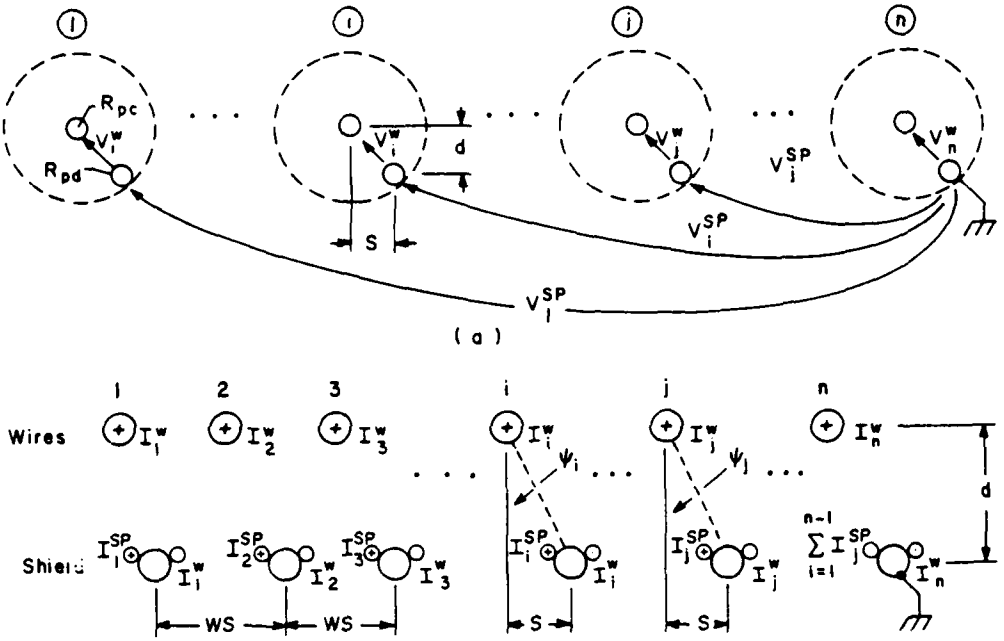

Figure 2.12 - Voltage and Current Definitions for the Pigtail Sections.

brought out to some type of connector to facilitate the connection of the cable to some device. This creates a section of exposed wires at each end of the cable, which will be referred to as the pigtail sections of the flatpack, coaxial cable.

The voltage and current definitions that are used in the derivation of the model are shown in Figure 2.12. We must use the same voltage and current vectors that were defined in (2-16) and (2-17) in the derivation to allow for the multiplication of the individual chain parameter matrices to form the total chain parameter matrix as previously discussed. As before we need to derive the per-unit-length line parameter matrices and then solve the MTL equations. The MTL equations can be written as follows for the pigtail section of the flatpack, coaxial cable [12]:

$$\begin{bmatrix} \underline{\dot{V}}^{w}(x) \\ \underline{\dot{V}}^{sp}(x) \end{bmatrix} = -(\underset{\sim}{Z}_{CP} + j\omega\underset{\sim}{L}_{P}) \begin{bmatrix} \underline{I}^{w}(x) \\ \underline{I}^{sp}(x) \end{bmatrix} \tag{2-42}$$

and

$$\begin{bmatrix} \underline{\dot{I}}^{w}(x) \\ \underline{\dot{I}}^{sp}(x) \end{bmatrix} = -j\omega\underset{\sim}{C}_{P} \begin{bmatrix} \underline{V}^{w}(x) \\ \underline{V}^{sp}(x) \end{bmatrix} \tag{2-43}$$

where $\underset{\sim}{Z}_{CP}$, $\underset{\sim}{L}_{P}$, and $\underset{\sim}{C}_{P}$ are the per-unit-length conductor impedance, inductance, and capacitance matrices of the pigtail section, respectively. Before we derive the per-unit-length parameter matrices for this section we will make the simplifying assumption that the pigtail conductors (both

where each of the submatrices are given by [12]

$$\underset{\sim}{\phi}^{s}_{11} = \tfrac{1}{2}\underset{\sim}{Y}_S^{-1}\underset{\sim}{T}\,(e^{\underset{\sim}{\gamma}\ell_s} + e^{-\underset{\sim}{\gamma}\ell_s})\,\underset{\sim}{T}^{-1}\,\underset{\sim}{Y}_S \qquad (2\text{-}41a)$$

$$\underset{\sim}{\phi}^{s}_{12} = -\tfrac{1}{2}\underset{\sim}{Y}_S\,\underset{\sim}{T}\,\underset{\sim}{\gamma}\,(e^{\underset{\sim}{\gamma}\ell_s} - e^{-\underset{\sim}{\gamma}\ell_s})\,\underset{\sim}{T}^{-1} \qquad (2\text{-}41b)$$

$$\underset{\sim}{\phi}^{s}_{21} = -\tfrac{1}{2}\,\underset{\sim}{T}\,(e^{\underset{\sim}{\gamma}\ell_s} - e^{-\underset{\sim}{\gamma}\ell_s})\,\underset{\sim}{\gamma}^{-1}\,\underset{\sim}{T}^{-1}\,\underset{\sim}{Y}_S \qquad (2\text{-}41c)$$

$$\underset{\sim}{\phi}^{s}_{22} = \tfrac{1}{2}\,\underset{\sim}{T}\,(e^{\underset{\sim}{\gamma}\ell_s} + e^{-\underset{\sim}{\gamma}\ell_s})\,\underset{\sim}{T}^{-1} \qquad (2\text{-}41d)$$

where $\underset{\sim}{Y}_S$ is defined to be $j\omega\underset{\sim}{C}_S$, $\underset{\sim}{T}$ is the n x n similarity transformation matrix which diagonalizes the $\underset{\sim}{Y}_S\underset{\sim}{Z}_S$ product as follows

$$\underset{\sim}{T}^{-1}\,\underset{\sim}{Y}_S\,\underset{\sim}{Z}_S\,\underset{\sim}{T} = \underset{\sim}{\gamma}^2$$

$\underset{\sim}{Z}_S$ is defined to be $\underset{\sim}{Z}_C + j\omega\underset{\sim}{L}_S$, $e^{\underset{\sim}{\gamma}\ell_s}$ and $e^{-\underset{\sim}{\gamma}\ell_s}$ are n x n diagonal matrices with entries $[e^{\underset{\sim}{\gamma}\ell_s}]_{ii} = e^{\gamma_i\ell_s}$ and $[e^{-\underset{\sim}{\gamma}\ell_s}]_{ii} = e^{-\gamma_i\ell_s}$.

From this derivation we are now able to calculate the chain parameter matrix of the shielded section of the flatpack, coaxial cable. We must now derive the chain parameter matrix of the pigtail sections to be able to calculate the total chain parameter matrix of the flatpack, coaxial cable.

2.3 - MULTICONDUCTOR TRANSMISSION LINE MODEL FOR THE PIGTAIL SECTIONS OF THE LINE

In this section, we wish to derive the multiconductor transmission line model for the pigtail sections of the flatpack, coaxial cable [13]. These sections come about because of the need to be able to terminate the ends of the individual coaxial cables. In general, wires are connected to the inner conductors and the edges of the shields and

coaxial cable as n "fat wires" due to the electrostatic shielding of the solid shields. Instead of calculating each of these terms as we did for the inductance matrix we can note that the surrounding medium is homogeneous so $\underset{\sim}{L}^{spsp}\underset{\sim}{C}^{spsp} = 1/v^2$ where v is the speed of light in the medium (in our case free-space)[12]. Since this must be true we can state that

$$\underset{\sim}{C}^{spsp} = \frac{1}{v^2}\underset{\sim}{L}^{spsp^{-1}} \tag{2-39}$$

where $()^{-1}$ represents the matrix inverse.

Now that we have calculated the entries of the per-unit-length parameter matrices, $\underset{\sim}{Z}_C$, $\underset{\sim}{L}_S$, and $\underset{\sim}{C}_S$, for the shielded section of the line we must turn our attention to solving the equations stated in (2-18)

$$\underline{V}(x) = -(\underset{\sim}{Z}_C + j\omega\underset{\sim}{L}_S)\ \underline{I}(x)$$

and

$$\underline{I}(x) = -j\omega\underset{\sim}{C}_S\ \underline{V}(x)$$

and obtaining the chain parameter matrix of the shielded section. These have been solved in general in [12] for sinusoidal steady-state excitation of the transmission line under the TEM mode assumption, and the results are repeated here. The chain parameter matrix for the shielded section can be calculated as

$$\underset{\sim}{\Phi}_S = \begin{bmatrix} \underset{\sim}{\Phi}^S_{11} & \underset{\sim}{\Phi}^S_{12} \\ \underset{\sim}{\Phi}^S_{21} & \underset{\sim}{\Phi}^S_{22} \end{bmatrix} \tag{2-40}$$

inductance for this situation. The first, l_1, is due to the current flowing down the j^{th} shield pigtail and can be calculated as

$$l_1 = -\frac{\mu_o}{2\pi} \ln\left(\frac{d_1}{d_2}\right) \tag{2-57}$$

The second contribution, l_2, is due to that current returning on the n^{th} shield pigtail and can be calculated as

$$l_2 = -\frac{\mu_o}{2\pi} \ln\left(\frac{d_3}{d_4}\right) \tag{2-58}$$

The four distances needed for this situation can be calculated as

$$d_1 = \sqrt{[((j - i) \times WS) + s)]^2 + d^2}$$

$$d_2 = (j - i) \times WS$$

$$d_3 = \sqrt{[((n - i) \times WS) + s)]^2 + d^2}$$

$$d_4 = (n - i) \times WS$$

Substituting these four distances into equations (2-57) and (2-58) and summing them to get the total inductance yields

$$l_{\substack{ij \\ j>i}} = -\frac{\mu_o}{2\pi} \ln\left[\frac{\sqrt{[((j - i) \times WS) + s)]^2 + d^2}}{(j - i) \times WS}\right] + \frac{\mu_o}{2\pi} \ln\left[\frac{\sqrt{[((n - i) \times WS) + s)]^2 + d^2}}{(n - i) \times WS}\right]$$

which reduces to

$$l_{\substack{ij \\ j>i}} = \frac{\mu_o}{2\pi} \ln\left[\frac{(j - i)\sqrt{[((n - i) \times WS) + s)]^2 + d^2}}{(n - i)\sqrt{[((j - i) \times WS) + s)]^2 + d^2}}\right] \tag{2-59}$$

Next we will calculate the terms of the $\underset{\sim}{L}^{wsp}$ submatrix

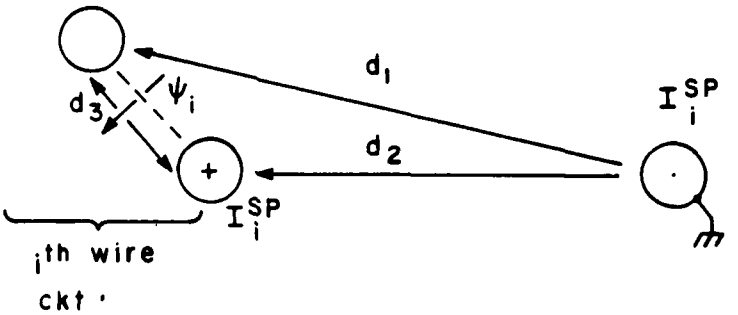

Figure 2.17 - Mutual Inductance Between the i^{th} Wire Circuit and the i^{th} Shield Circuit over the Pigtail Sections.

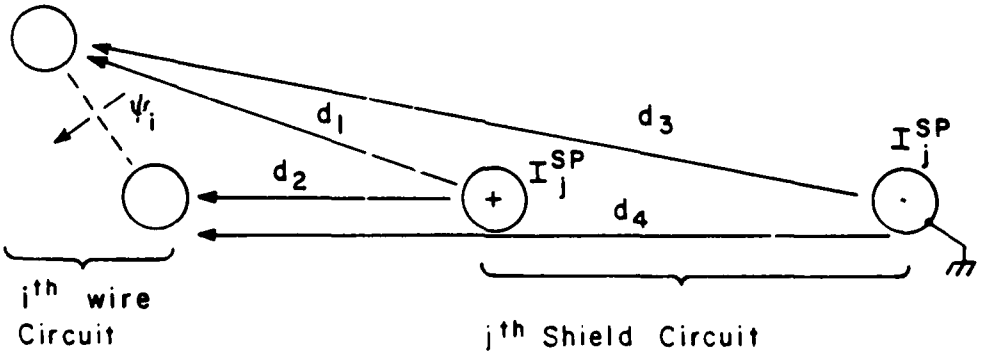

Figure 2.18 - Mutual Inductance Between the i^{th} Wire Circuit and the j^{th} Shield Circuit over the Pigtail Sections.

that lie in region 2 of (2-53). For this region of the submatrix i > j and its corresponding representation is shown in Figure 2.19. Again there are two contributions to the net inductance that must be calculated. The first, l_1, is due to the current flowing down the j^{th} shield pigtail and can be calculated as

$$l_1 = \frac{\mu_o}{2\pi} \ln\left(\frac{d_2}{d_1}\right) \qquad (2\text{-}60)$$

The second contribution, l_2, is due to the current returning on the n^{th} shield pigtail and can be calculated as

$$l_2 = \frac{\mu_o}{2\pi} \ln\left(\frac{d_3}{d_4}\right) \qquad (2\text{-}61)$$

The four distances needed to solve equations (2-60) and (2-61) can be calculated as

$$d_1 = \sqrt{[((i - j) \times WS) - s)]^2 + d^2}$$

$$d_2 = (i - j) \times WS$$

$$d_3 = \sqrt{[((n - i) \times WS) + s)]^2 + d^2}$$

$$d_4 = (n - i) \times WS$$

Substituting these four distances into equations (2-60) and (2-61) and summing them to get the total inductance yields

$$l_{\substack{ij \\ i>j}} = \frac{\mu_o}{2\pi} \ln\left[\frac{(i - j) \times WS}{\sqrt{[((i - j) \times WS) - s)]^2 + d^2}}\right] + \frac{\mu_o}{2\pi} \ln\left[\frac{\sqrt{[((n - i) \times WS) + s)]^2 + d^2}}{(n - i) \times WS}\right]$$

which reduces to

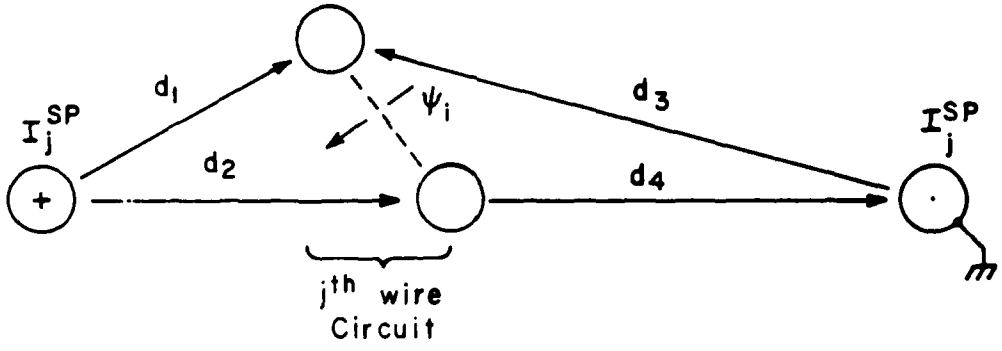

Figure 2.19 - Mutual Inductance Between the j^{th} Shield Circuit and the i^{th} Wire Circuit over the Pigtail Sections.

$$l_{\substack{ij \\ i>j}} = \frac{\mu_o}{2\pi} \ln \left[\frac{(i - j) \sqrt{[((n - i) \times WS) + s)]^2 + d^2}}{(n - i) \sqrt{[((i - j) \times WS) + s)]^2 + d^2}} \right] \quad (2\text{-}62)$$

Finally we must calculate the entries of the L^{wsp} submatrix that lie in region 3 of (2-53). For this region of the submatrix i=n and its corresponding representation is shown in Figure 2.20. Again there are two contributions to the net inductance for this situation. The first, l_1, is due to the current flowing down the j^{th} shield pigtail and can be

$$l_1 = \frac{\mu_o}{2\pi} \ln \left(\frac{d_2}{d_1} \right) \quad (2\text{-}63)$$

The second contribution, l_2, is due to the current returning on the n^{th} shield pigtail and can be calculated as

$$l_2 = \frac{\mu_o}{2\pi} \ln \left(\frac{d_3}{R_{pd}} \right) \quad (2\text{-}64)$$

The three distances needed for this situation can be calculated as

$$d_1 = \sqrt{[((n - j) \times WS) - s)]^2 + d^2}$$

$$d_2 = (n - j) \times WS$$

$$d_3 = \sqrt{d^2 + s^2}$$

Substituting these three distances into equations (2-63) and (2-64) and summing them to get the total inductance yields

$$l_{nj} = \frac{\mu_o}{2\pi} \ln \left[\frac{(n - j) \times WS}{\sqrt{[((n - j) \times WS) - s)]^2 + d^2}} \right] + \frac{\mu_o}{2\pi} \ln \left[\frac{\sqrt{d^2 + s^2}}{R_{pd}} \right]$$

which reduces to

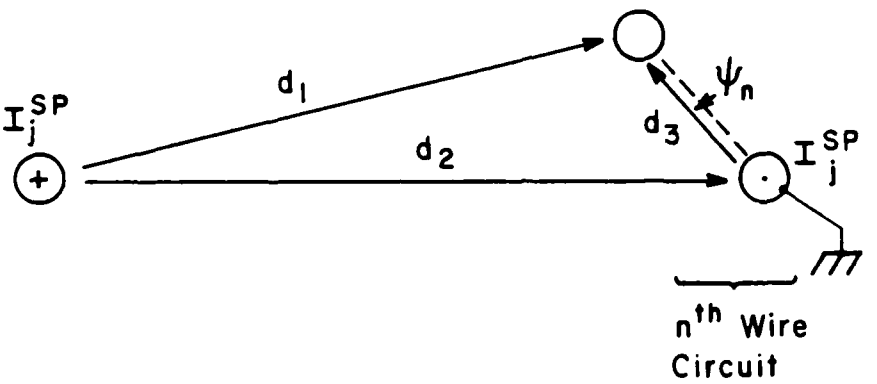

Figure 2.20 - Mutual Inductance Between the j^{th} Shield Circuit and the n^{th} Wire Circuit over the Pigtail Sections.

$$l_{nj} = \frac{\mu_o}{2\pi} \ln \left[\frac{(n - j) \times WS \times \sqrt{d^2 + s^2}}{\sqrt{[((n - j) \times WS) - s)]^2 + d^2} \times R_{pd}} \right] \quad (2\text{-}65)$$

Finally we need to calculate the L^{spw} submatrix of L_p. This submatrix could be calculated directly but instead we will use the argument presented previously stating that due to the surrounding medium being reciprocal the per-unit-length parameter matrices must be symmetric. For this to be true the following condition must be true

$$\underset{\sim}{L}^{spw} = (\underset{\sim}{L}^{wsp})^t \quad (2\text{-}66)$$

We have now calculated all the entries in the per-unit-length inductance matrix, $\underset{\sim}{L}_p$, of the pigtail sections. Now we will calculate the per-unit-length capacitance matrix, $\underset{\sim}{C}_p$, of the pigtail sections. Instead of calculating the entries of this matrix we note that since the medium surrounding the pigtails (free space) is homogeneous, the following condition must hold [12]

$$\underset{\sim}{L}_p \, \underset{\sim}{C}_p = 1/v^2$$

where v is the speed of light in the medium. Since this must be true we can state that

$$\underset{\sim}{C}_p = 1/v^2 \, (\underset{\sim}{L}_p)^{-1} \quad (2\text{-}67)$$

Now that we have calculated the entries of the per-unit-length parameter matrices, $\underset{\sim}{L}_p$ and $\underset{\sim}{C}_p$, for the pigtail sections of the flatpack, coaxial cable we must solve the equations stated in (2-18)

$$\underline{V}(x) = -(\underset{\sim}{Z}_C + j\omega\underset{\sim}{L}_P)\ \underline{I}(x)$$

and

$$\underline{I}(x) = -j\omega\underset{\sim}{C}_P\ \underline{V}(x)$$

and obtain the chain parameter matrix of the pigtail sections. These equations have been solved in general for sinusoidal, steady-state excitation of the line under the TEM mode assumption in [12]. The results are repeated here for convenience. The chain parameter matrix for the pigtail sections can be calculated as

$$\underset{\sim}{\Phi}_P = \begin{bmatrix} \underset{\sim}{\phi}^P_{11} & \underset{\sim}{\phi}^P_{12} \\ \underset{\sim}{\phi}^P_{21} & \underset{\sim}{\phi}^P_{22} \end{bmatrix} \qquad (2\text{-}68)$$

where each of the submatrices are given by

$$\underset{\sim}{\phi}^P_{11} = \cos(\beta\,\ell_P)\ \underset{\sim}{1}_{2n-1} \qquad (2\text{-}69a)$$

$$\underset{\sim}{\phi}^P_{12} = -jv\,\sin(\beta\,\ell_P)\ \underset{\sim}{L}_P \qquad (2\text{-}69b)$$

$$\underset{\sim}{\phi}^P_{21} = -jv\,\sin(\beta\,\ell_P)\ \underset{\sim}{C}_P \qquad (2\text{-}69c)$$

$$\underset{\sim}{\phi}^P_{22} = \cos(\beta\,\ell_P)\ \underset{\sim}{1}_{2n-1} \qquad (2\text{-}69d)$$

where β, the wave number, is given by $\beta = 2\pi / \lambda$, $\lambda = v/f$, $v = 1/\sqrt{\mu_o\varepsilon_o}$ and $\underset{\sim}{1}_{2n-1}$ represents the (2n-1 x 2n-1) identity matrix.

2.4 - TOTAL CHAIN PARAMETER MATRIX OF THE FLATPACK, COAXIAL CABLE

In the previous two sections we have derived equations that make it possible to calculate the chain parameter matrices of the shielded section and each of the pigtail sections that are present at each end of the flatpack, coaxial cable. These chain parameter matrices can be

calculated for various configurations of the flatpack, coaxial cable by substituting in the correct values of the various line parameters (R_{pd}, R_{shd}, s, d, etc.) for the given configuration. Once these individual chain parameter matrices have been calculated we can obtain the total chain parameter matrix using equation (2-10) presented in section 2.1.

As stated previously, once we have the total chain parameter matrix, $\underset{\sim}{\Phi}_T$, we have an equation which only relates the voltages and currents at each end of the flatpack, coaxial cable. To solve explicitly for the terminal voltages and currents of the line we must incorporate the terminal conditions of the line into the equations. This is done in the next section.

2.5 - INCORPORATING THE TERMINAL CONDITIONS

We will assume that the flatpack, coaxial cable is terminated at each end as shown in Figure 2.21. This termination configuration allows for connection of a load resistance and a voltage source at each end of the individual coaxial cables. Each of the individual wire circuits ground may be connected to the reference conductor by setting the corresponding R_{GLi} or R_{GRi} shown in the figure to zero. The overall chain parameter matrix of the entire line (including the pigtail sections) is given in (2-12) as

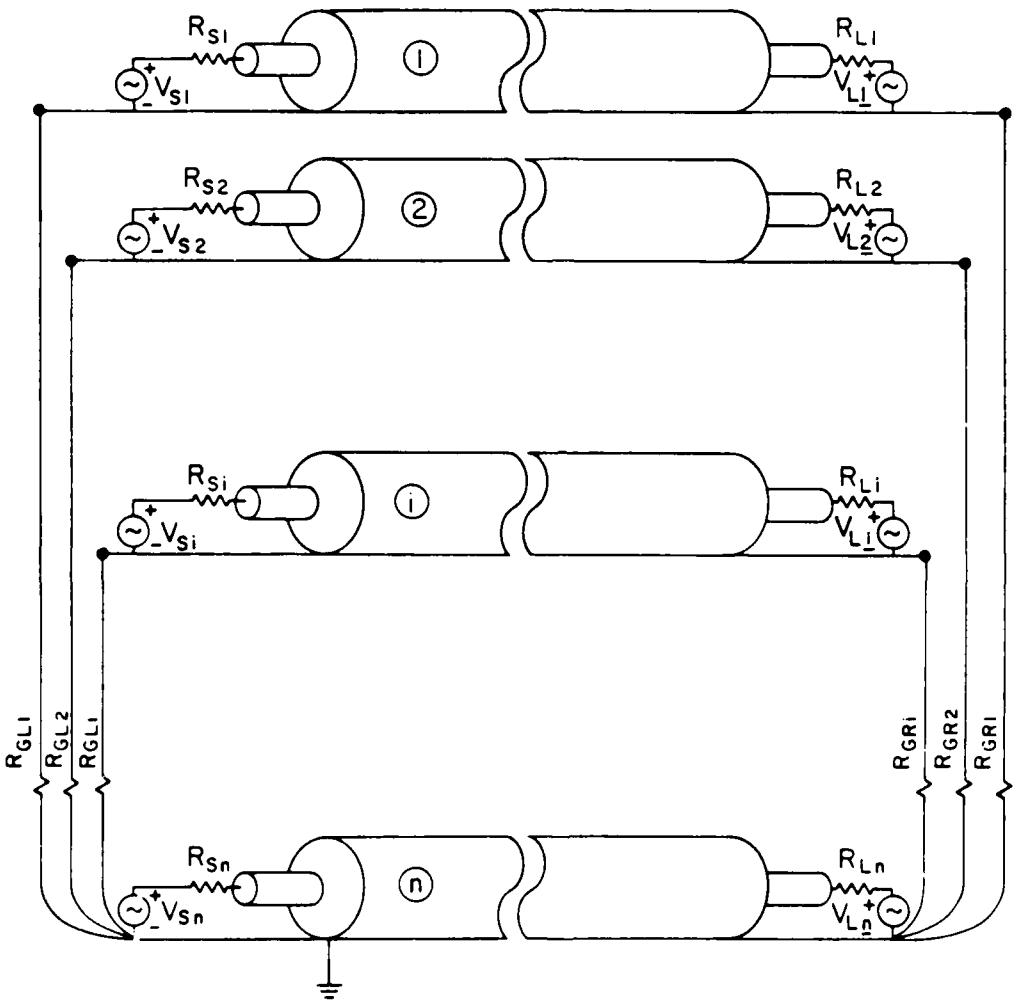

Figure 2.21 - Terminal Characterization.

$$\begin{bmatrix} V_R \\ \underline{I}_R \end{bmatrix} = \begin{bmatrix} & \underset{\sim}{\Phi}_T & \end{bmatrix} \begin{bmatrix} V_L \\ \underline{I}_L \end{bmatrix}$$

where

$$\underset{\sim}{\Phi}_T = \begin{bmatrix} \phi_{11}^T & \phi_{12}^T \\ \phi_{21}^T & \phi_{22}^T \end{bmatrix}$$

This equation can be rewritten as

$$\begin{bmatrix} \underline{V}_R^w \\ V_R^{sp} \\ \underline{I}_R^w \\ \underline{I}_R^{sp} \end{bmatrix} = \begin{bmatrix} \underset{\sim}{\Phi}_{11} & \underset{\sim}{\Phi}_{12} & \underset{\sim}{\Phi}_{13} & \underset{\sim}{\Phi}_{14} \\ \underset{\sim}{\Phi}_{21} & \underset{\sim}{\Phi}_{22} & \underset{\sim}{\Phi}_{23} & \underset{\sim}{\Phi}_{24} \\ \underset{\sim}{\Phi}_{31} & \underset{\sim}{\Phi}_{32} & \underset{\sim}{\Phi}_{33} & \underset{\sim}{\Phi}_{34} \\ \underset{\sim}{\Phi}_{41} & \underset{\sim}{\Phi}_{42} & \underset{\sim}{\Phi}_{43} & \underset{\sim}{\Phi}_{44} \end{bmatrix} \begin{bmatrix} V_L^w \\ V_L^{sp} \\ \underline{I}_L^w \\ \underline{I}_L^{sp} \end{bmatrix} \quad (2\text{-}70)$$

For the experimental configuration to be described in the next chapter, all the shields were grounded together, i.e., $R_{GRi} = R_{GLi} = 0$ for i=1,2,...,n-1. Although more general shield grounding configurations could have been investigated it is anticipated that this grounding configuration will be quite typical. For the terminal configuration shown in Figure 2.21 with all the shields grounded we can write a generalized Thevenin equivalent representation as

$$\underline{V}_L = V_S(0) - \underset{\sim}{Z}_0 \underline{I}_L \quad (2\text{-}71)$$

for the left end of the cable and

$$\underline{V}_R = V_S(\ell) + \underset{\sim}{Z}_\ell \underline{I}_R \quad (2\text{-}72)$$

for the right end of the cable where we have the following matrix definitions

$$\underline{V}_S(0) = \begin{bmatrix} \underline{V}_S^W(0) \\ \underline{0} \end{bmatrix} \text{ where } \underline{V}_S^W(0) = \begin{bmatrix} V_{S1} \\ V_{S2} \\ \vdots \\ V_{Sn} \end{bmatrix} \tag{2-73}$$

$$\underline{V}_S(\ell) = \begin{bmatrix} \underline{V}_S^W(\ell) \\ \underline{0} \end{bmatrix} \text{ where } \underline{V}_S^W(\ell) = \begin{bmatrix} V_{L1} \\ V_{L2} \\ \vdots \\ V_{Ln} \end{bmatrix} \tag{2-74}$$

$$Z_0 = \begin{bmatrix} \underset{\sim}{R}(0) & \underset{\sim}{0} \\ \underset{\sim}{0} & \underset{\sim}{0} \end{bmatrix} \text{where } \underset{\sim}{R}(0) = \begin{bmatrix} R_{S1} & & \\ & R_{S2} & \\ & & \ddots \\ & & & R_{Sn} \end{bmatrix} \tag{2-75}$$

$$Z_\ell = \begin{bmatrix} \underset{\sim}{R}(\ell) & \underset{\sim}{0} \\ \underset{\sim}{0} & \underset{\sim}{0} \end{bmatrix} \text{where } R(\ell) = \begin{bmatrix} R_{L1} & & \\ & R_{L2} & \\ & & \ddots \\ & & & R_{Ln} \end{bmatrix} \tag{2-76}$$

By solving the equations (2-12), (2-71), and (2-72) it will be possible to determine the terminal voltages and currents at each end of the cable. These equations have been solved in general in [12] for $\underline{I}_L$ and $\underline{I}_R$. The equation that solves for $\underline{I}_L$ is [12]

$$[\underset{\sim}{Z}_\ell \underset{\sim}{\phi}_{22}^T - \underset{\sim}{Z}_\ell \underset{\sim}{\phi}_{21}^T \underset{\sim}{Z}_0 - \underset{\sim}{\phi}_{12}^T + \underset{\sim}{\phi}_{11}^T \underset{\sim}{Z}_0] \underline{I}_L =$$
$$[\underset{\sim}{\phi}_{11}^T - \underset{\sim}{Z}_\ell \underset{\sim}{\phi}_{21}^T] \underline{V}_S(0) - \underline{V}_S(\ell) \tag{2-77}$$

By relating (2-70) to (2-12) we can make the following

observations

$$\underset{\sim}{\Phi}_{11}^{T} = \begin{bmatrix} \underset{\sim}{\Phi}_{11} & \underset{\sim}{\Phi}_{12} \\ \underset{\sim}{\Phi}_{21} & \underset{\sim}{\Phi}_{22} \end{bmatrix} \tag{2-78a}$$

$$\underset{\sim}{\Phi}_{12}^{T} = \begin{bmatrix} \underset{\sim}{\Phi}_{13} & \underset{\sim}{\Phi}_{14} \\ \underset{\sim}{\Phi}_{23} & \underset{\sim}{\Phi}_{24} \end{bmatrix} \tag{2-78b}$$

$$\underset{\sim}{\Phi}_{21}^{T} = \begin{bmatrix} \underset{\sim}{\Phi}_{31} & \underset{\sim}{\Phi}_{32} \\ \underset{\sim}{\Phi}_{41} & \underset{\sim}{\Phi}_{42} \end{bmatrix} \tag{2-78c}$$

$$\underset{\sim}{\Phi}_{22}^{T} = \begin{bmatrix} \underset{\sim}{\Phi}_{33} & \underset{\sim}{\Phi}_{34} \\ \underset{\sim}{\Phi}_{43} & \underset{\sim}{\Phi}_{44} \end{bmatrix} \tag{2-78d}$$

Calculating all the terms we need to solve (2-77) by substituting for all the entries gives

$$\underset{\sim}{Z}_{\mathcal{L}} \underset{\sim}{\Phi}_{22}^{T} = \begin{bmatrix} \underset{\sim}{R}(\mathcal{L}) & \underset{\sim}{0} \\ \underset{\sim}{0} & \underset{\sim}{0} \end{bmatrix} \begin{bmatrix} \underset{\sim}{\Phi}_{33} & \underset{\sim}{\Phi}_{34} \\ \underset{\sim}{\Phi}_{43} & \underset{\sim}{\Phi}_{44} \end{bmatrix} = \begin{bmatrix} \underset{\sim}{R}(\mathcal{L}) \underset{\sim}{\Phi}_{33} & \underset{\sim}{R}(\mathcal{L}) \underset{\sim}{\Phi}_{34} \\ \underset{\sim}{0} & \underset{\sim}{0} \end{bmatrix} \tag{2-79}$$

$$\underset{\sim}{Z}_{\mathcal{L}} \underset{\sim}{\Phi}_{21}^{T} \underset{\sim}{Z}_{0} = \begin{bmatrix} \underset{\sim}{R}(\mathcal{L}) & \underset{\sim}{0} \\ \underset{\sim}{0} & \underset{\sim}{0} \end{bmatrix} \begin{bmatrix} \underset{\sim}{\Phi}_{31} & \underset{\sim}{\Phi}_{32} \\ \underset{\sim}{\Phi}_{41} & \underset{\sim}{\Phi}_{42} \end{bmatrix} \begin{bmatrix} \underset{\sim}{R}(0) & \underset{\sim}{0} \\ \underset{\sim}{0} & \underset{\sim}{0} \end{bmatrix} =$$

$$= \begin{bmatrix} \underset{\sim}{R}(\mathcal{L}) & \underset{\sim}{0} \\ \underset{\sim}{0} & \underset{\sim}{0} \end{bmatrix} \begin{bmatrix} \underset{\sim}{\Phi}_{31} \underset{\sim}{R}(0) & \underset{\sim}{0} \\ \underset{\sim}{\Phi}_{41} \underset{\sim}{R}(0) & \underset{\sim}{0} \end{bmatrix} = \begin{bmatrix} \underset{\sim}{R}(\mathcal{L}) \underset{\sim}{\Phi}_{31} \underset{\sim}{R}(0) & \underset{\sim}{0} \\ \underset{\sim}{0} & \underset{\sim}{0} \end{bmatrix} \tag{2-80}$$

$$\underset{\sim}{\Phi}_{11}^{T} \underset{\sim}{Z}_{0} = \begin{bmatrix} \underset{\sim}{\Phi}_{11} & \underset{\sim}{\Phi}_{12} \\ \underset{\sim}{\Phi}_{21} & \underset{\sim}{\Phi}_{22} \end{bmatrix} \begin{bmatrix} \underset{\sim}{R}(0) & \underset{\sim}{0} \\ \underset{\sim}{0} & \underset{\sim}{0} \end{bmatrix} = \begin{bmatrix} \underset{\sim}{\Phi}_{11} \underset{\sim}{R}(0) & \underset{\sim}{0} \\ \underset{\sim}{0} & \underset{\sim}{0} \end{bmatrix} \tag{2-81}$$

$$\underset{\sim}{Z}_{\ell}\,\underset{\sim}{\Phi}_{21}^{T} = \begin{bmatrix} \underset{\sim}{R}(\ell) & \underset{\sim}{0} \\ \underset{\sim}{0} & \underset{\sim}{0} \end{bmatrix} \begin{bmatrix} \underset{\sim}{\Phi}_{31} & \underset{\sim}{\Phi}_{32} \\ \underset{\sim}{\Phi}_{41} & \underset{\sim}{\Phi}_{42} \end{bmatrix} = \begin{bmatrix} \underset{\sim}{R}(\ell)\,\underset{\sim}{\Phi}_{31} & \underset{\sim}{R}(\ell)\,\underset{\sim}{\Phi}_{32} \\ \underset{\sim}{0} & \underset{\sim}{0} \end{bmatrix} \tag{2-82}$$

Substituting (2-79), (2-80), (2-81), (2-82), (2-78a), and (2-78b) into (2-77) yields

$$\left\{ \begin{bmatrix} \underset{\sim}{R}(\ell)\,\underset{\sim}{\Phi}_{33} & \underset{\sim}{R}(\ell)\,\underset{\sim}{\Phi}_{34} \\ \underset{\sim}{0} & \underset{\sim}{0} \end{bmatrix} - \begin{bmatrix} \underset{\sim}{R}(\ell)\,\underset{\sim}{\Phi}_{31}\,\underset{\sim}{R}(0) & \underset{\sim}{0} \\ \underset{\sim}{0} & \underset{\sim}{0} \end{bmatrix} - \begin{bmatrix} \underset{\sim}{\Phi}_{13} & \underset{\sim}{\Phi}_{14} \\ \underset{\sim}{\Phi}_{23} & \underset{\sim}{\Phi}_{24} \end{bmatrix} + \begin{bmatrix} \underset{\sim}{\Phi}_{11}\,\underset{\sim}{R}(0) & \underset{\sim}{0} \\ \underset{\sim}{0} & \underset{\sim}{0} \end{bmatrix} \right\} \underline{I}_L =$$

$$= \left\{ \begin{bmatrix} \underset{\sim}{\Phi}_{11} & \underset{\sim}{\Phi}_{12} \\ \underset{\sim}{\Phi}_{21} & \underset{\sim}{\Phi}_{22} \end{bmatrix} - \begin{bmatrix} \underset{\sim}{R}(\ell)\,\underset{\sim}{\Phi}_{31} & \underset{\sim}{R}(\ell)\,\underset{\sim}{\Phi}_{32} \\ \underset{\sim}{0} & \underset{\sim}{0} \end{bmatrix} \right\} \underline{V}_S(0) - \underline{V}(\ell)$$

which reduces to

$$\left[\begin{array}{cc} \underset{\sim}{R}(\ell)\,\underset{\sim}{\Phi}_{33} - \underset{\sim}{R}(\ell)\,\underset{\sim}{\Phi}_{31}\underset{\sim}{R}(0) - \underset{\sim}{\Phi}_{13} + \underset{\sim}{\Phi}_{11}\underset{\sim}{R}(0) & \underset{\sim}{R}(\ell)\,\underset{\sim}{\Phi}_{34} - \underset{\sim}{\Phi}_{14} \\ - \underset{\sim}{\Phi}_{23} + \underset{\sim}{\Phi}_{21}\,\underset{\sim}{R}(0) & - \underset{\sim}{\Phi}_{24} \end{array}\right] \underline{I}_L =$$

$$= \left[\begin{array}{cc} \underset{\sim}{\Phi}_{11} - \underset{\sim}{R}(\ell)\,\underset{\sim}{\Phi}_{31} & \underset{\sim}{\Phi}_{12} - \underset{\sim}{R}(\ell)\,\underset{\sim}{\Phi}_{32} \\ \underset{\sim}{\Phi}_{21} & \underset{\sim}{\Phi}_{22} \end{array}\right] \underline{V}_S(0) - \underline{V}_S(\ell) \tag{2-83}$$

Everything in equation (2-83) is known except $\underline{I}_L$ therefore we can solve the equation for $\underline{I}_L$ from which we can calculate the terminal voltages at the left end of the cable by substitution of $\underline{I}_L$ into equation (2-71). We can now solve for $\underline{I}_R$ using $\underline{I}_L$ as shown in [12] as

$$\underline{I}_R = -[\underset{\sim}{\Phi}_{21}^{T}\,\underset{\sim}{Z}_0 - \underset{\sim}{\Phi}_{22}^{T}]\;\underline{I}_L + \underset{\sim}{\Phi}_{21}^{T}\,\underline{V}_S(0) \tag{2-84}$$

Substituting (2-78c), (2-78d), and $\underset{\sim}{Z}_0$ into this equation we get

$$V_C = \frac{(Z_C)\ (V_G)}{Z_{OG} + Z_{IG}} \tag{3-2}$$

This voltage divides across the loads at each end of the receptor wire to give

$$V_{OR} = \frac{Z_{OR}}{Z_{OR} + Z_{IR}}\ V_C \tag{3-3}$$

and

$$V_{IR} = -\ \frac{Z_{IR}}{Z_{OR} + Z_{IR}}\ V_C \tag{3-4}$$

These induced voltages, V_{OR} and V_{IR}, are independent of frequency for the frequency range being considered.

We will calculate the level of common impedance coupling that should exist for our experimental setup. If we substitute equation (3-2) into (3-3) and divide through by the driving voltage, V_G, we obtain

$$\frac{V_{OR}}{V_G} = \left(\frac{Z_{OR}}{Z_{OR} + Z_{IR}}\right)\left(\frac{Z_C}{Z_{OG} + Z_{IG}}\right) \tag{3-5}$$

where V_{OR}/V_G is the level of common impedance coupling present. The impedances at each end of the receptor wire are the 91 Ω resistors that terminate each of the cables so

$$Z_{OR} = Z_{IR} = 91\,\Omega \tag{3-6}$$

The load at the far end of the generator wire is, again, a 91 Ω resistor so

$$Z_{IG} = 91\,\Omega \tag{3-7}$$

We will assume for our calculations that

$$Z_{OG} = 0 \tag{3-8}$$

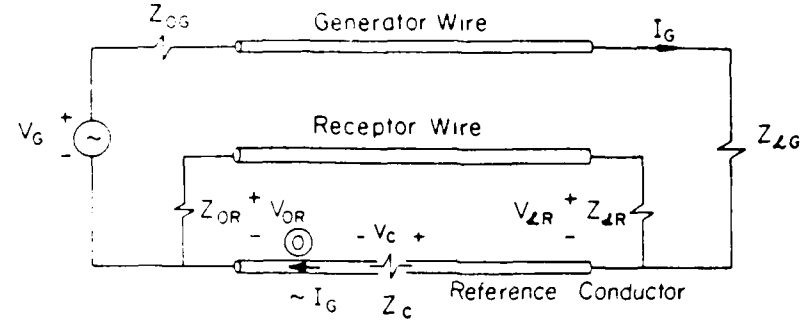

(a)

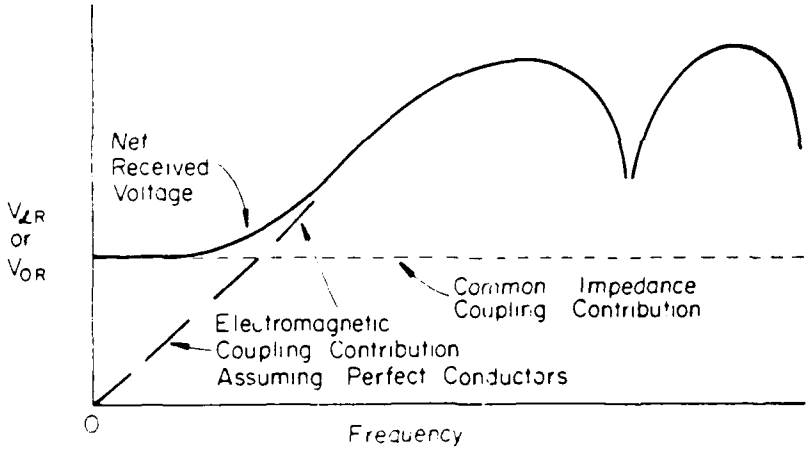

(b)

Figure 3.7 - Common Impedance Coupling.

occur.

To illustrate the concept of common impedance coupling consider Figure 3.7(a). We drive one of the wires shown with some voltage, V_G, and wish to know what effect this has on the load voltages in the system. For the case of our flatpack, coaxial cable, cable 1 can be thought of as the generator wire and the cable we are presently observing (2, 7, or 13) can be thought of as the receptor wire. The common return, since all 13 shields are shorted together, is all 13 of the shields in parallel.

If we drive the generator wire with a voltage, V_G, then a current, I_G, will flow in the generator wire circuit and ,for a sufficiently small frequency, can be calculated as

$$I_G = \frac{V_G}{Z_{OG} + Z_{1G}} \qquad (3\text{-}1)$$

This current will flow through the common return, whose impedance is denoted as Z_C. This reference conductor impedance is a distributed parameter phenomenon, but for the frequencies being considered, the line is electrically short and we may lump this impedance at a single point. This current will produce a voltage across the reference conductor, V_C, which can be calculated as

$$V_C = Z_C I_G$$

which is equal to

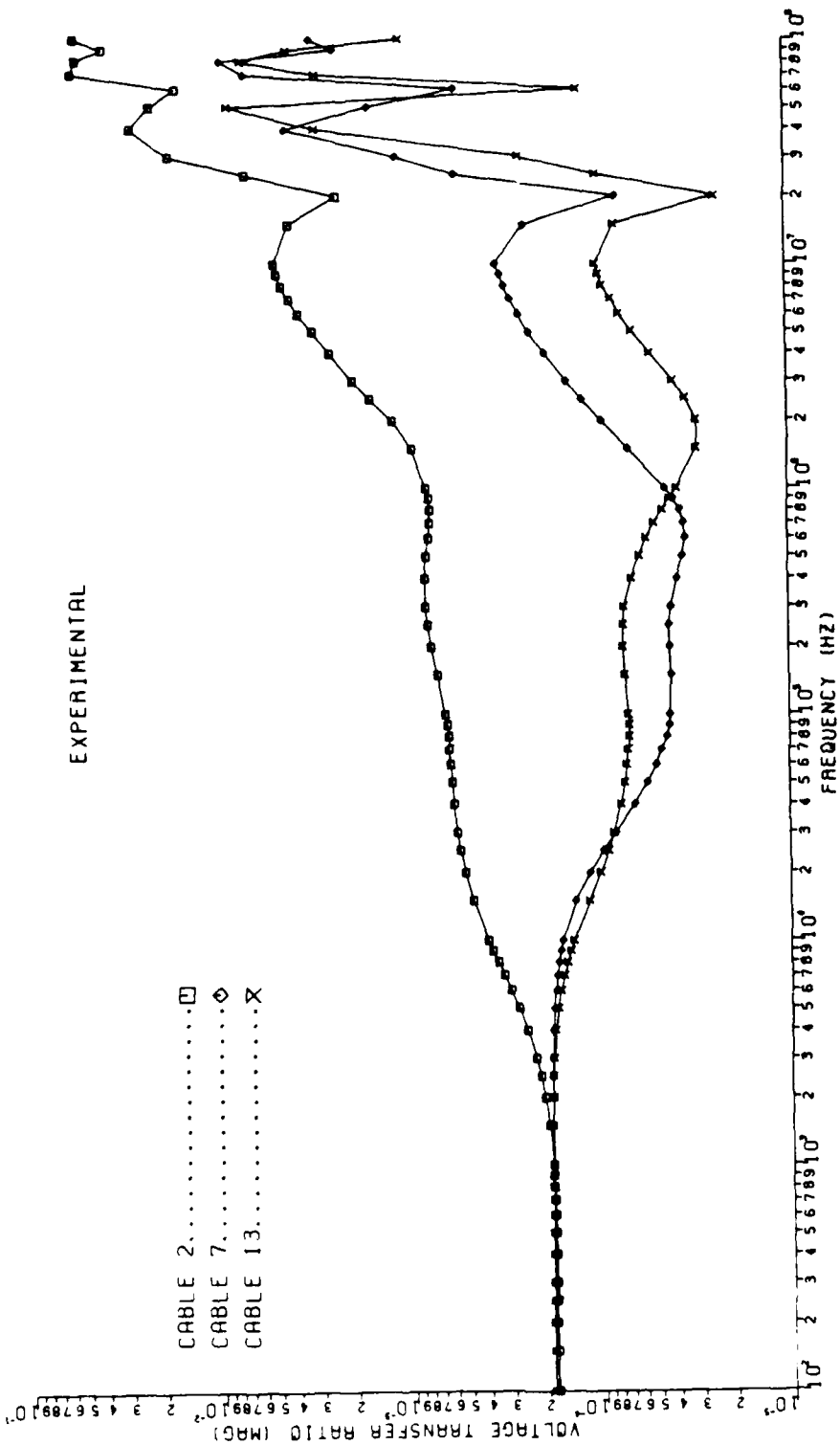

Figure 3.6 - Comparison of Experimental Results for Crosstalk to Cables 2, 7, and 13.

$$\frac{V_2}{V_{in}}, \quad \frac{V_7}{V_{in}}, \text{ and } \frac{V_{13}}{V_{in}}$$

Each transfer ratio has a magnitude and a phase; we will only consider their magnitudes denoted as $|\cdot|$.

The measurements described above were performed for frequencies ranging from 100 Hz to 100 MHz in steps of 1, 1.5, 2, 2.5, 3, 4, 5, 6, 7, 8, and 9 in each decade. The results of these measurements are shown in Figure 3.6 where we have plotted the magnitudes of the voltage transfer ratios for cables 2, 7, and 13 versus frequency.

3.2 - ANALYSIS OF EXPERIMENTAL RESULTS

In this section we will qualitatively describe the crosstalk behavior exhibited by the flatpack, coaxial cable over various frequency ranges of the graph shown in Figure 3.6. The first section of the graph we will consider is the portion for which the frequency is less than 1 KHz. In this range the crosstalk is constant and approximately equal to 1.8×10^{-4} for all three of the cables. This type of coupling is usually observable at low frequencies and is known as common impedance coupling. It is present in circuits in which two or more individual circuits share a common return, which is the case for our experimental setup of the flatpack, coaxial cable. All 13 of the individual coaxial cable circuits share the 13^{th} shield as their return therefore we can expect this type of coupling to

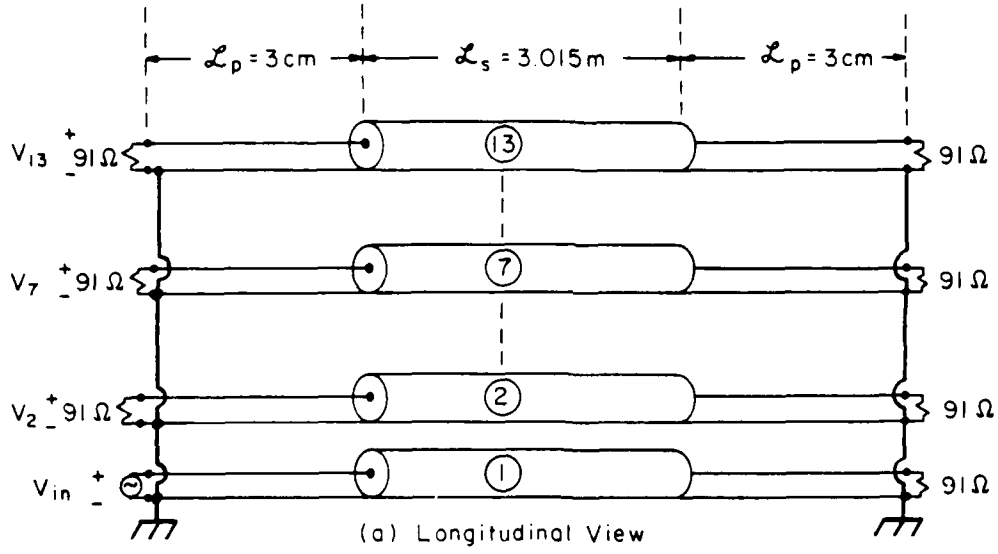

Figure 3.5 - Line Characterization.

between the ends of the terminating resistors and the beginning of the shielded section. This distance was measured to be 3.0×10^{-2} meters.

To measure the levels of crosstalk present in the cable, each end of each of the individual coaxial cables was terminated to ground with a resistor whose value equals the characteristic impedance of the cable (91Ω) with the exception of cable 1's left(near) end. The left(near) end of cable 1 was then driven with a sinusoidal voltage source, v_{in}, and the voltages induced on various cables were measured to allow for the calculation of the actual levels of crosstalk present in the cable. From the dimensions given previously we can calculate the characteristic impedance of each of the individual cables to be 91Ω. The cables were terminated with 91Ω resistors as depicted in Figure 3.5 and pictured in Figure 3.2.

Three of the coaxial cables in the flatpack cable were arbitrarily chosen for measurement of the induced voltages, cables 2, 7, and 13. We are able to measure the voltage transfer ratios(i.e., level of crosstalk) to the left(near) ends of each of the chosen cables by placing a known v_{in} at the left(near) end of cable 1 and then measuring the voltages present at the left(near) ends of cables 2, 7, and 13 denoted v_2, v_7, and v_{13}, respectively. The transfer ratios can then be calculated as

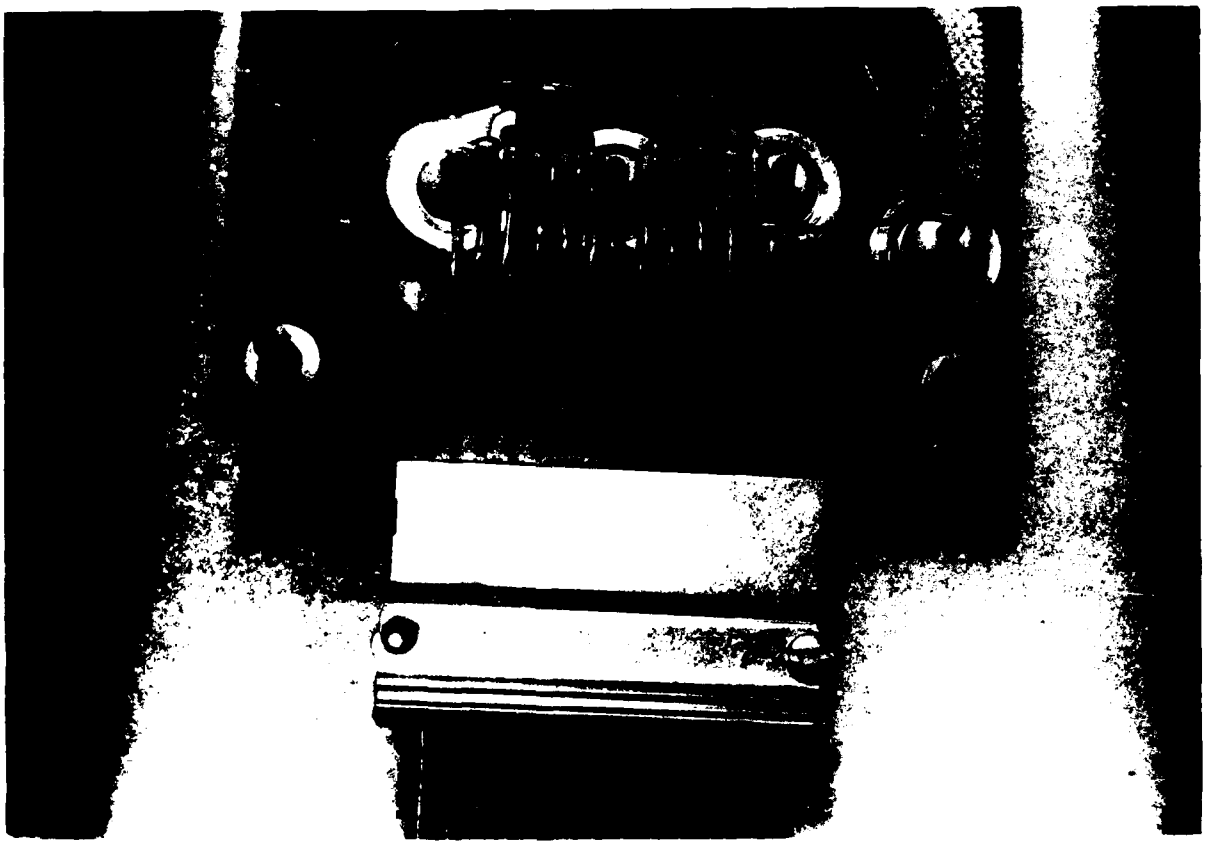

Figure 3.4 - Cable Termination.

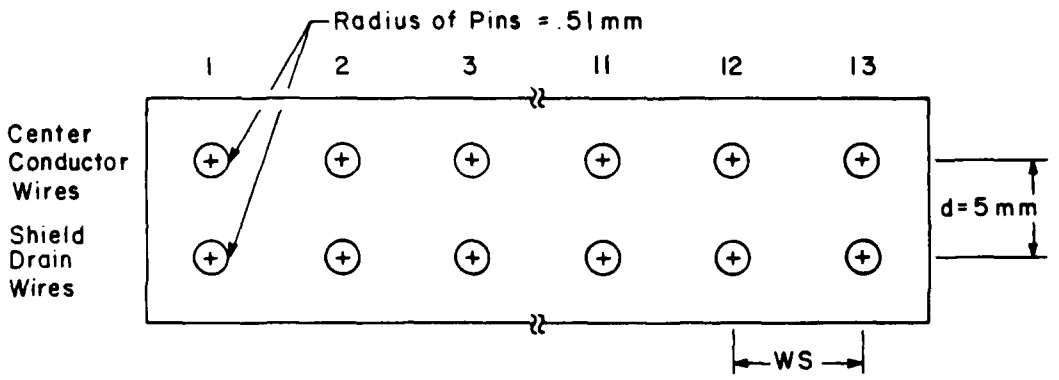

Figure 3.3 - Connector Dimensions.

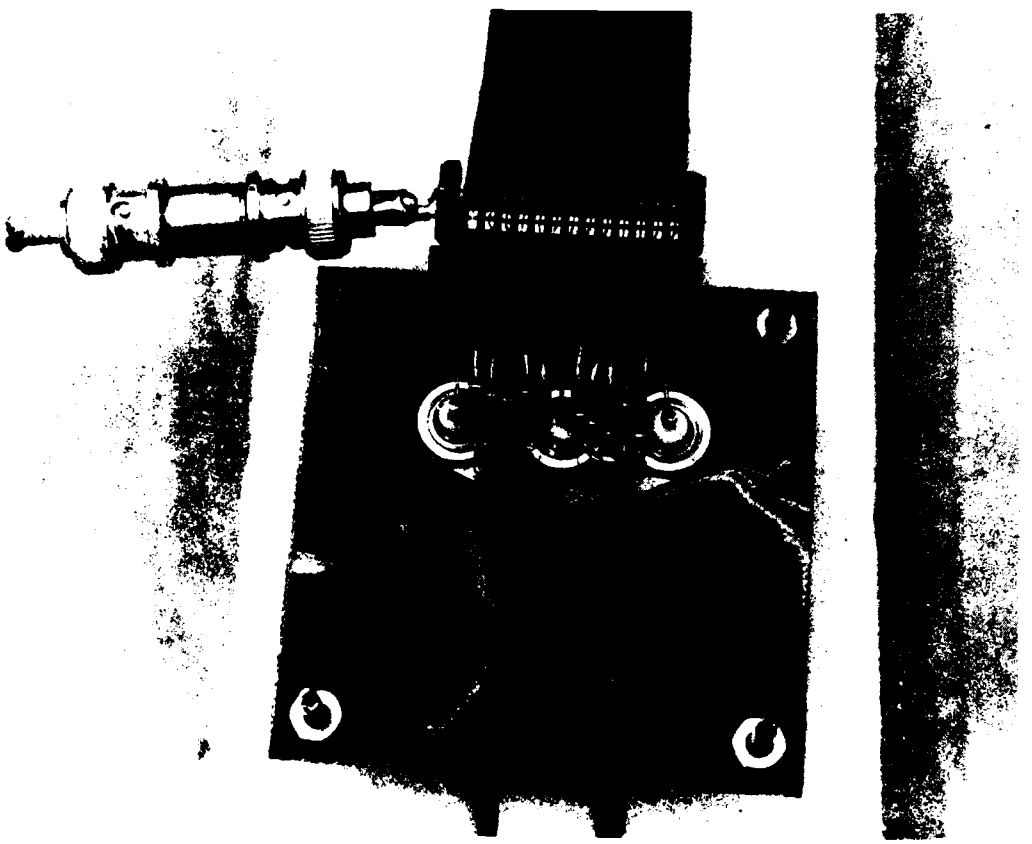

Figure 3.2 - Cable Connector.

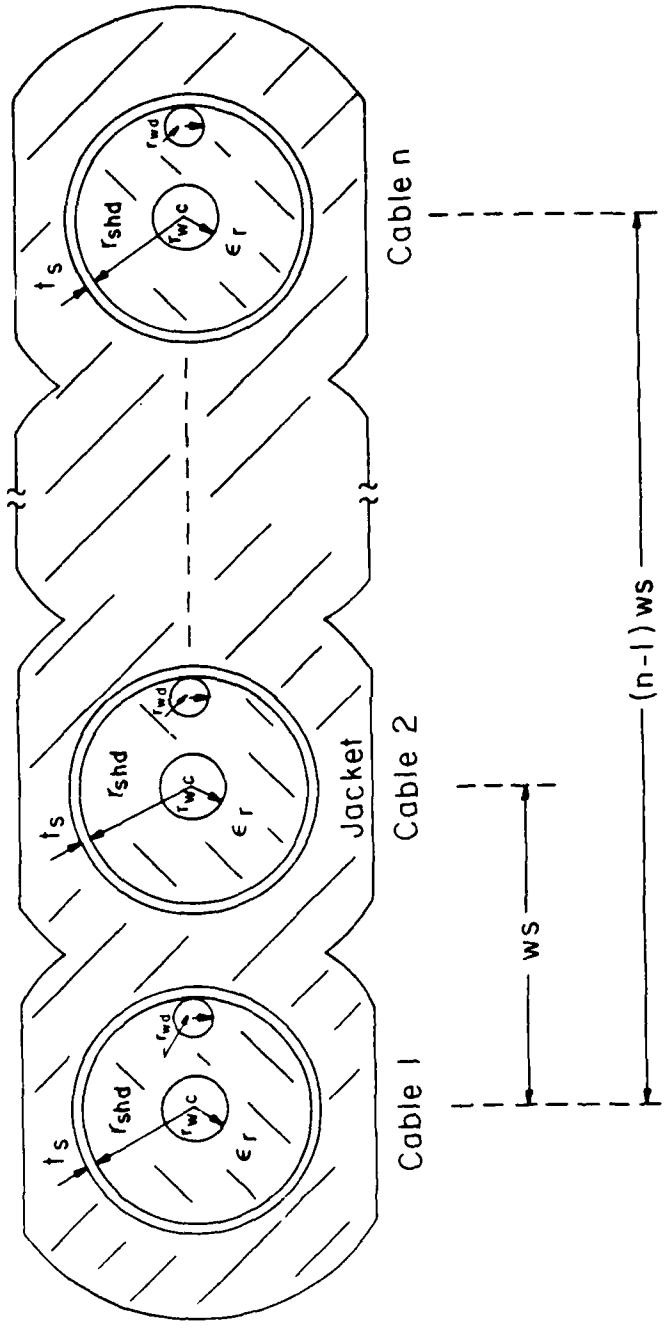

Figure 3.1 - Flatpack, Coaxial Cable.

denoted as having radius R_{wd} is a wire that runs the length of the cable and is pressed against the interior surface of the shield to allow for electrical connection to the shields.

The cable is terminated at each end with Amp 226477-1 receptacle connectors [14] to allow for connection to each of the individual coaxial cables of the flatpack, coaxial cable. These connectors contain 26 pins, 13 for the center wires and 13 for the drain wires that connect to the individual coaxial shields. One of these connectors is shown in Figure 3.2 with pertinent connector dimensions being shown in Figure 3.3.

The pigtail sections discussed in Chapter 2 come about in the connector terminations at the ends of the cable. To allow for connection to the center wires and drain wires of the flatpack, coaxial cable, these wires are extended past the end of the shielded section and connector to the pins of the terminating connectors. This can be more closely observed in Figure 3.4. The dimensions of the pigtail sections with reference to Figure 2.12 are

$$R_{pc} = .51 \times 10^{-3} \text{ meters}$$

$$R_{pd} = .51 \times 10^{-3} \text{ meters}$$

$$WS = 2.54 \times 10^{-3} \text{ meters}$$

$$s = 0 \text{ meters}$$

$$d = 5.0 \times 10^{-3}$$

The length of the pigtail sections, ℓ_p, is the distance

CHAPTER 3

EXPERIMENTAL RESULTS vs. COMPUTED RESULTS

The purpose of this chapter is to compare experimental measurements of the levels of electromagnetic crosstalk present in a typical flatpack, coaxial cable to predictions made by a digital computer program that implements the model of the flatpack, coaxial cable derived in Chapter 2. From these results we will judge whether or not we can use the model to simulate the crosstalk present in this class of cables.

3.1 - THE EXPERIMENT

The cable chosen for the experimental work was an Amp 1-226464-3 flatpack, coaxial cable which has 13 individual coaxial cables [14]. The cross-sectional dimensions of the cable with reference to Figure 3.1 are:

$WS = 100$ mils (2.54×10^{-3} meters)

$R_{shd} = 32$ mils (8.128×10^{-4} meters)

$t_s = .35$ mils (8.89×10^{-6} meters)

$R_{wc} = 5$ mils (1.27×10^{-4} meters)

$R_{wd} = 6.3$ mils (1.6×10^{-4} meters)

$\varepsilon_r = 1.5$ (foamed polyethylene)

The length of the shielded sections of the cable, ℓ_s, is 3.015 meters. The drain wire shown in Figure 3.1 and

$$\underline{I}_R = -\left\{ \begin{bmatrix} \underset{\sim}{\Phi}_{31} & \underset{\sim}{\Phi}_{32} \\ \underset{\sim}{\Phi}_{41} & \underset{\sim}{\Phi}_{42} \end{bmatrix} \begin{bmatrix} \underset{\sim}{R}(0) & \underset{\sim}{0} \\ \underset{\sim}{0} & \underset{\sim}{0} \end{bmatrix} - \begin{bmatrix} \underset{\sim}{\Phi}_{33} & \underset{\sim}{\Phi}_{34} \\ \underset{\sim}{\Phi}_{43} & \underset{\sim}{\Phi}_{44} \end{bmatrix} \right\} \underline{I}_L + \begin{bmatrix} \underset{\sim}{\Phi}_{31} & \underset{\sim}{\Phi}_{32} \\ \underset{\sim}{\Phi}_{41} & \underset{\sim}{\Phi}_{42} \end{bmatrix} \underline{V}_S(0)$$

which reduces to

$$\underline{I}_R = \left[\begin{array}{c|c} \underset{\sim}{\Phi}_{33} - \underset{\sim}{\Phi}_{31}\,\underset{\sim}{R}(0) & \underset{\sim}{\Phi}_{34} \\ \hline \underset{\sim}{\Phi}_{43} - \underset{\sim}{\Phi}_{41}\,\underset{\sim}{R}(0) & \underset{\sim}{\Phi}_{44} \end{array} \right] \underline{I}_L + \begin{bmatrix} \underset{\sim}{\Phi}_{31} & \underset{\sim}{\Phi}_{32} \\ \underset{\sim}{\Phi}_{41} & \underset{\sim}{\Phi}_{42} \end{bmatrix} \underline{V}_S(0) \qquad (2\text{-}85)$$

Everything on the right-hand side of equation (2-85) is known therefore we can solve for $\underline{I}_R$ from which we can calculate the terminal voltages at the right end of the cable by substitution of $\underline{I}_R$ into equation (2-72).

We have now derived a set of matrix equations, (2-83) and (2-85), which may be used to calculate the terminal voltages at each end of the cable given the line characteristics and terminal characteristics. It is possible to predict the amount of electromagnetic crosstalk between two cables in the flatpack, coaxial cable by "driving" one of the wires with a known voltage and then calculating the voltage that would be present on the other wire. The crosstalk would then be equal to the ratio of these two voltages. This approach will be taken in the next chapter to attempt to predict the crosstalk present in a given flatpack, coaxial cable. To test the accuracy of the predictions, they will be compared to actual experimental measurements.

The only value needed to solve equation (3-5) is the value of the resistance of the common return, Z_C. This value is simply the value of 13 shields in parallel which can be written as

$$Z_C = \frac{1}{13} Z_{SH} \tag{3-9}$$

where Z_{SH} denotes the resistance of a single shield.

To calculate Z_{SH} we first look at the construction of an individual shield, shown in Figure 3.8. The shields consist of a .35 mil thickness of aluminum bonded to a 1 mil thickness of mylar. Each circular shield is formed in a "cigarette wrapper" form as shown. The impedance of one of these shields can be calculated as

$$Z_{SH} = \frac{\ell_S}{\sigma \, w \, t_s} \tag{3-10}$$

where σ is the conductivity of the shield (aluminum, i.e., $\sigma = 3.82 \times 10^7$), t_s is the thickness of the shield, and w is the width of the "rolled out" shield which was measured to be 270 mils. For our given cable we find that $Z_{SH} = 1.294641\Omega$ so that

$$Z_C = \frac{1}{13} Z_{SH} = .0995878 \ \Omega \tag{3-11}$$

Substituting the values given by (3-6), (3-7), (3-8), and (3-11) into equation (3-5) yields

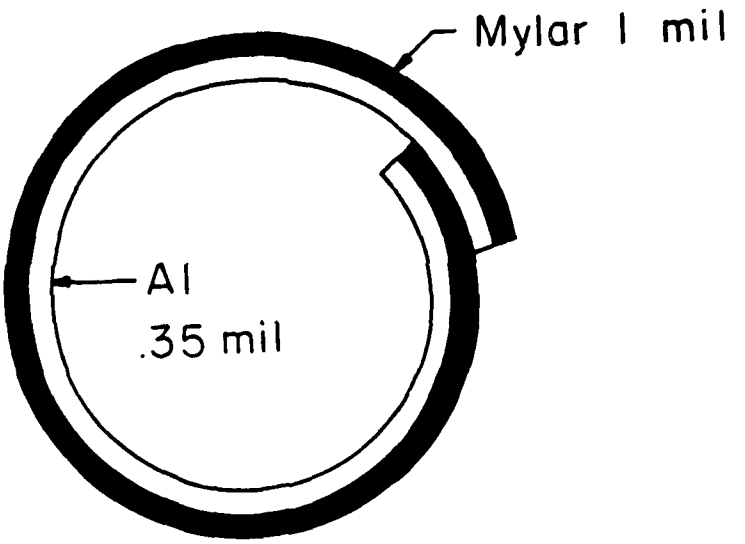

Figure 3.8 - Shield Construction.

$$\frac{V_{OR}}{V_G} = 5.472 \times 10^{-4} \qquad (3\text{-}12)$$

which is far from the measured value of the crosstalk 1.8×10^{-4}. The concept of common impedance coupling is widely used and known to be accurate[1]. Therefore we reconsider the formulation of V_{OR}/V_G. The values Z_{OR}, Z_{IR}, Z_{OG}, and Z_{IG} are fixed. The only place an error could occur is in our formulation of Z_C. The dc resistance of one of the shields was measured and found to be .4154Ω which is far from our calculated value of 1.294641Ω.

The "problem" with the shield impedance was investigated further. Looking back at Figure 3.1 one notes that each of the shields have a drain wire that runs the length of the cable and is in direct contact with the shield along that distance. This suggests that the impedance of the returns of each of the individual circuits should be modelled as a drain wire in parallel with the shield instead of just the impedance of the shield. The per-unit-length dc shield impedance, z_{SH}, is calculated as

$$z_{SH} = \frac{1}{\sigma w t_s} = .4294 \ \Omega/\text{meter} \qquad (3\text{-}13)$$

The per-unit-length drain wire impedance, z_D, can be calculated as

$$z_D = \frac{1}{\sigma_D \pi R_{wd}} = .2143 \ \Omega/\text{meter} \qquad (3\text{-}14)$$

where σ_D is the conductivity of the drain wire (in our case

copper). We can model the drain wire - shield impedance as N sections of length ℓ_S/N as shown in Figure 3.9(a). It can be mathematically proven that the circuit shown in Figure 3.9(a) is equivalent to the circuit shown in Figure 3.9(b) regardless of the value of N.

If we now calculate the dc impedance of the common return for all the circuits, which is 13 of these drain wire - shield combinations in parallel we obtain

$$z_C = \frac{(z_D \,||\, z_{SH})\ell_S}{13} = .033154\ \Omega \qquad (3\text{-}15)$$

where || stands for "in parallel with". If we substitute this new value of z_C into equation (3-5) with all other values as they were before we obtain

$$\frac{V_{OR}}{V_G} = 1.82 \times 10^{-4} \qquad (3\text{-}16)$$

which compare very favorably to the measured value of 1.8×10^{-4}. This implies that we must include the drain wire impedance in all calculations dealing with the shield impedance.

The next section of the graph shown in Figure 3.6 we wish to consider is the frequency range of 1 KHz to 1 MHz. Ideally when crosstalk is measured for transmission lines the voltage transfer ratio should begin at the level of the common impedance coupling, stay at that level for a range of frequencies, and then roll off at 20 dB/decade. If we

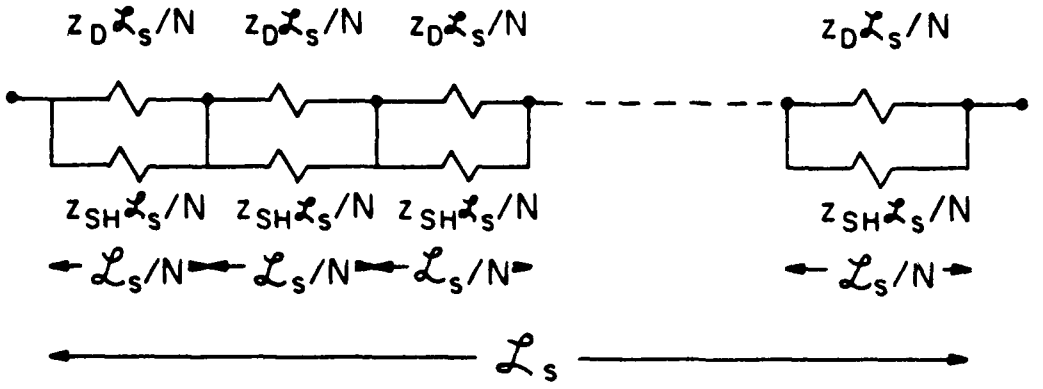

(a)

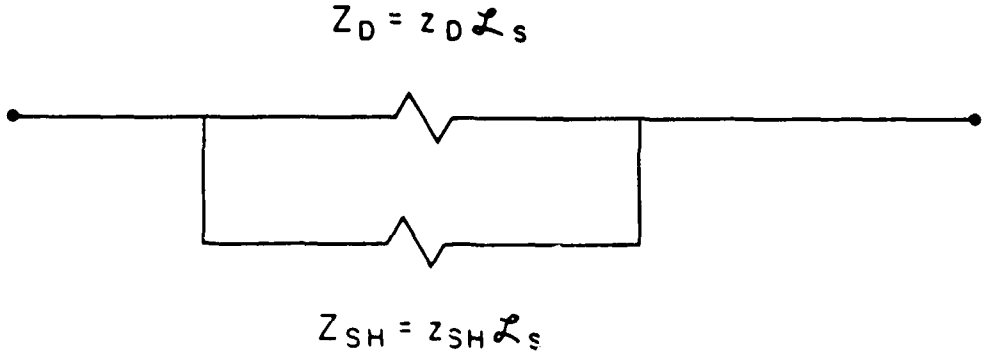

(b)

Figure 3.9 - Equivalent Circuit for the Shield - Drain Wire Combination.

look at Figure 3.6 we see that instead of rolling off at 20 dB/decade, cables 7 and 13 exhibit "bumps" around the frequency of 200 KHz and the voltage transfer ratio for cable 2 actually increases over this region. The shield impedance may, as before, account for this "strange" behavior of the voltage transfer ratio. The shield impedance was therefore measured for the frequency range of 100 Hz to 10 MHz. The results are shown in Figure 3.10. The shield - drain wire impedance was calculated for the same frequency range as stated above and those results also shown in Figure 3.10.

The shield wall (t_s = .35 mils) is one skin depth at 84 MHz which implies that the shield impedance (as well as the transfer impedance) should be relatively constant up to this frequency. To measure this impedance the flatpack cable was formed in a loop to allow for connection to the measuring equipment. At frequencies above 1 MHz the inductance of this loop will start to affect the impedance measurements therefore we cannot trust our measurements above this frequency. Below this range, however, our measurements seem to match the computed values very closely. If we look at the computed impedance of the drain wire - shield combination we notice that its impedance starts to increase at approximately 200 KHz, the exact same frequency that the "bumps" occurred in the voltage transfer ratio. It will be shown later that this increase in the

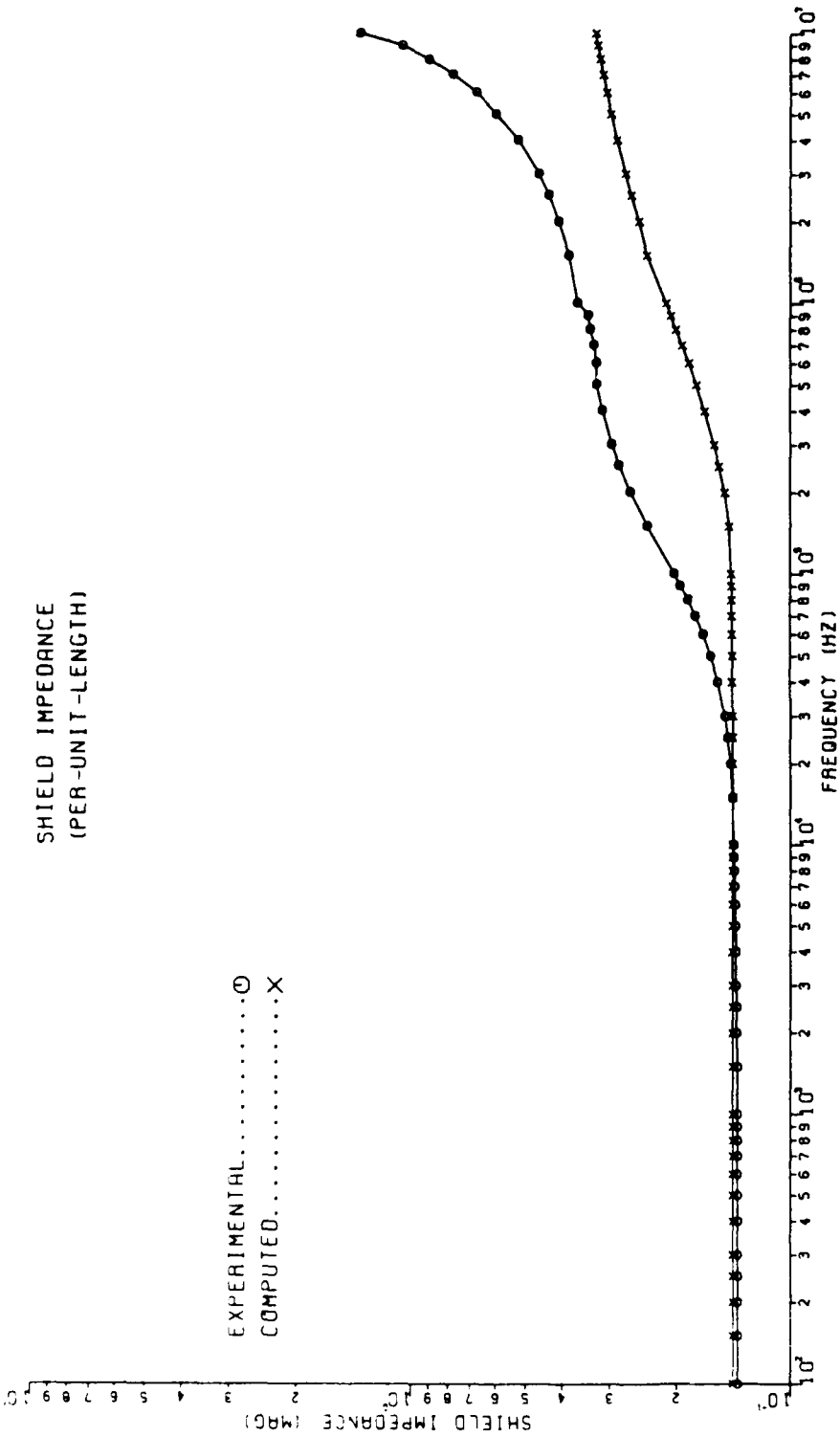

Figure 3.10 - Measured and Computed Shield Impedance.

impedance does, in fact, account for the "bumps" that occur in the voltage transfer ratios. To verify this increasing of the shield impedance, independent measurements of the shield impedance of a similiar cable were made in a quadraxial test fixture [16]. The results showed the same trend as our experimental data.

The next portion of the graph shown in Figure 3.6 that we consider is that for which the frequency is in the range of 1 MHz to 10 MHz. Over this region the crosstalk begins to increase at a rate of 20 dB/decade. This is due solely to the exposed pigtail sections in the connectors. This point is addressed in more detail in [4,13]. Basically these documents show that for an electrically short line, the coupling that occurs over the shielded section and the coupling that occurs over the the pigtail sections can be superimposed. The coupling over the shielded section should either remain constant or roll off as frequency increases. The coupling over the pigtail sections, however, is increasing at 20 dB/decade [4,13]. Thus there exists a frequency at which the pigtail coupling level will begin to dominate the overall coupling. This occurs at approximately 1 MHz for our configuration.

To further illustrate the pigtail effect, the driving wire pigtail was removed from the connectors at each end of the cable, and cable 1 driven precisely at the input of the

shielded section. This should eliminate most of the direct coupling over the pigtail section. Some secondary coupling will still exist due to the pigtails of the undriven wires but it should be small in comparison to the coupling with the driving pigtail wire present. The crosstalk for cables 2, 7, and 13 were remeasured with the driving pigtail wire removed and the results are shown in Figures 3.11, 3.12, and 3.13. Note that removing the driven wire from the pigtail section has reduced the crosstalk by over 20 dB which confirms the pigtail effect.

The final portion of the graph shown in Figure 3.6 that we need to consider is that portion for which the frequency is greater than 10 MHz. Over this frequency range the line is becoming electrically long. It is expected that prediction of the crosstalk over this range would be difficult but will be shown later that the model derived in Chapter 2 does fairly accurately predict the levels of crosstalk in this region.

3.3 - THE TRANSMISSION LINE MODEL

A digital computer program (FLATCOAX) was written to implement the multiconductor transmission line model of the flatpack, coaxial cable which was derived in Chapter 2. The use of this program will be described in Chapter 5. The program reads input data that consist of the line dimensions, pertinent dimensions of the pigtail sections,

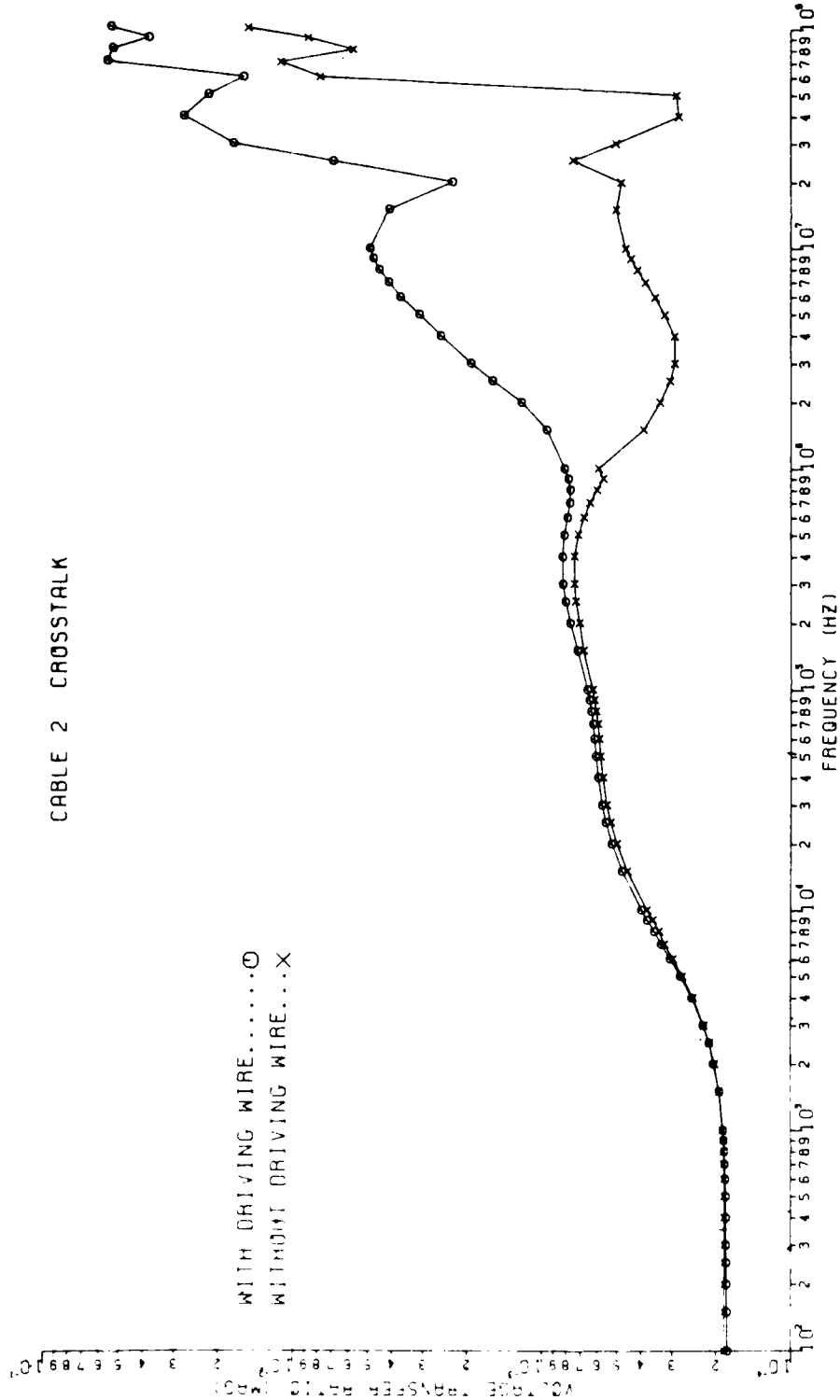

Figure 3.11 - Effect of Pigtail Sections on Cable 2's Crosstalk.

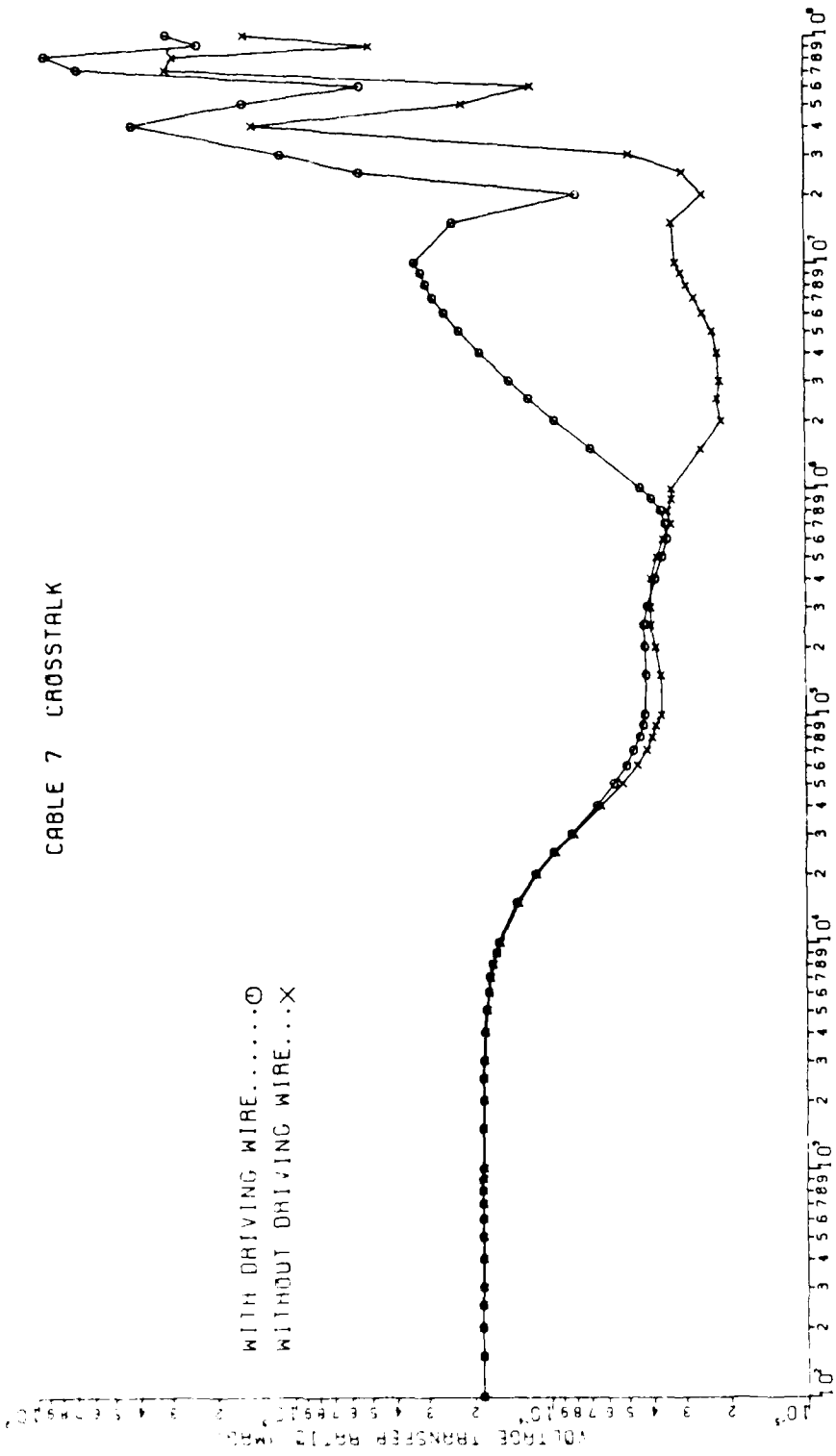

Figure 3.12 - Effect of Pigtail Sections on Cable 7's Crosstalk.

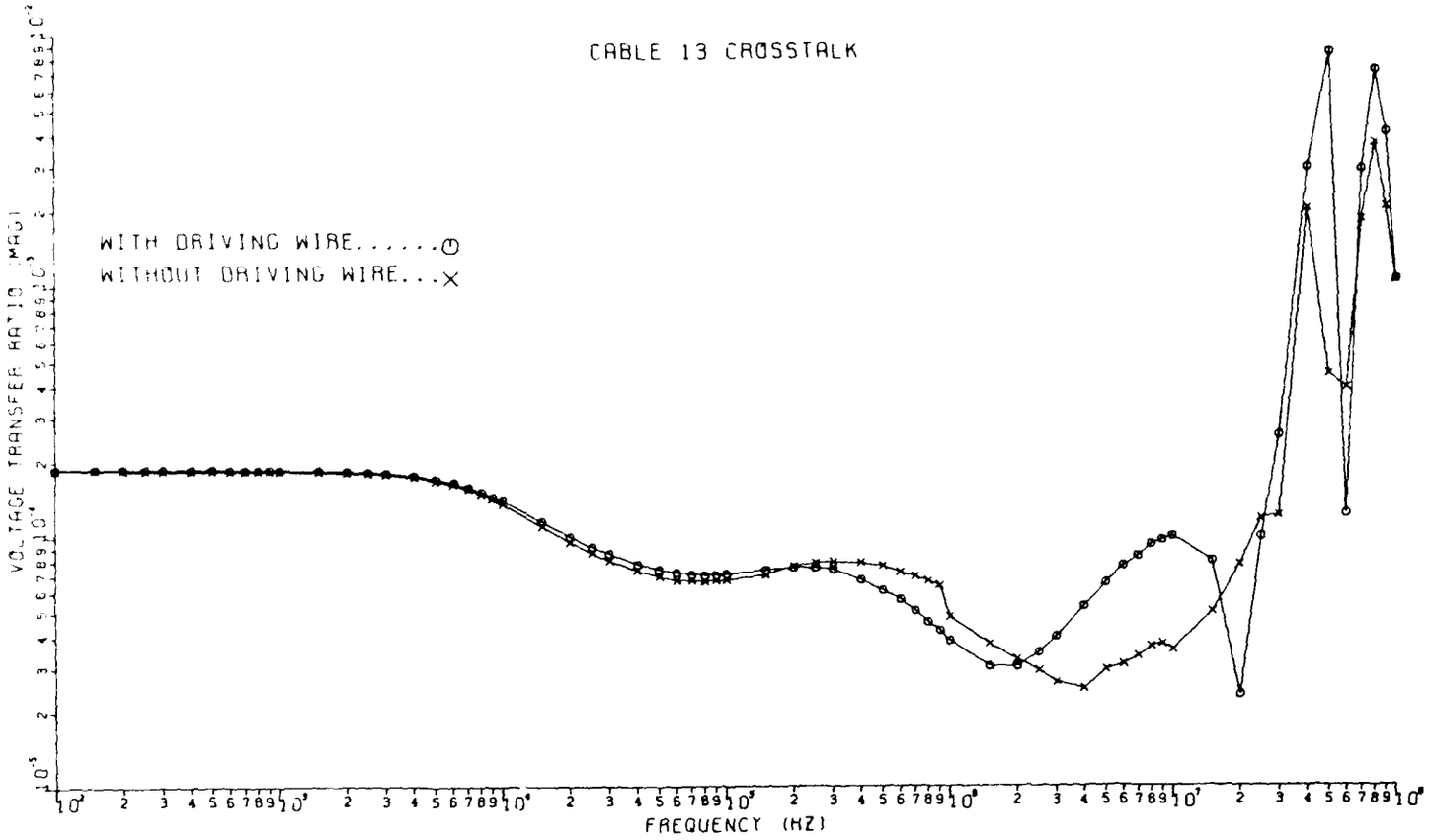

Figure 3.13 - Effect of Pigtail Sections on Cable 13's Crosstalk.

terminal characteristics, and desired frequency of computation. It then computes the overall chain parameter matrix for the described cable, incorporates the terminal conditions, and solves for the terminal voltages at each end of the listed frequencies.

The predicted levels of crosstalk for cables 2, 7, and 13 are plotted along with their experimental values in Figures 3.14, 3.15, and 3.16. Note that the predictions are generally quite satisfactory. For frequencies above 10 MHz, the line is becoming electrically long, as stated previously, and accurate predictions in this range are more difficult.

Due to the favorable correlation between the computed and experimental results we can conclude that it is possible to accurately predict the crosstalk present in a flatpack, coaxial cable using the method derived in Chapter 2. To illustrate the large variation in crosstalk levels within the flatpack, coaxial cable, the predictions of the crosstalk for all 13 cables at the near and far ends of the cable are shown in Figures 3.17 and 3.18. Note that there is a maximum difference in crosstalk levels between individual coaxial cables in the flatpack cable of as much as [illegible] dB.

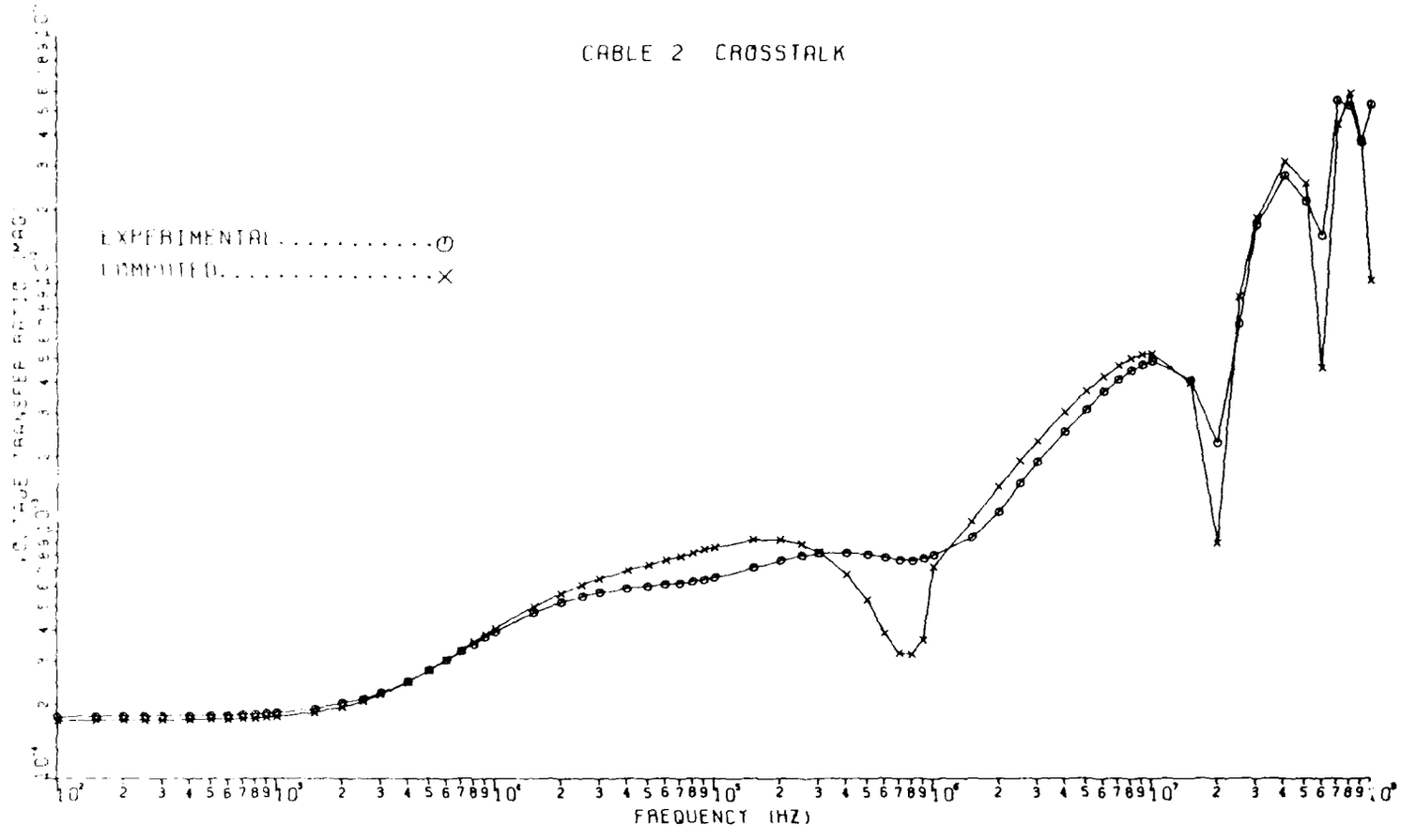

Figure 3.14 - Predicted versus Experimental Results for Cable 2.

AD-A153 111 BASIC EMC TECHNOLOGY ADVANCEMENT FOR C3 SYSTEMS VOLUME 2/2
4F PREDICTION OF C.. (U) SOUTHEASTERN CENTER FOR
ELECTRICAL ENGINEERING EDUCATION INC S..
UNCLASSIFIED W E BEECH ET AL. DEC 84 F/G 9/3 NL

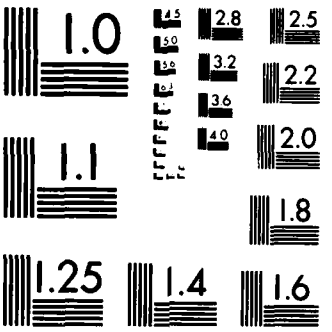

MICROCOPY RESOLUTION TEST CHART
NATIONAL BUREAU OF STANDARDS-1963-A

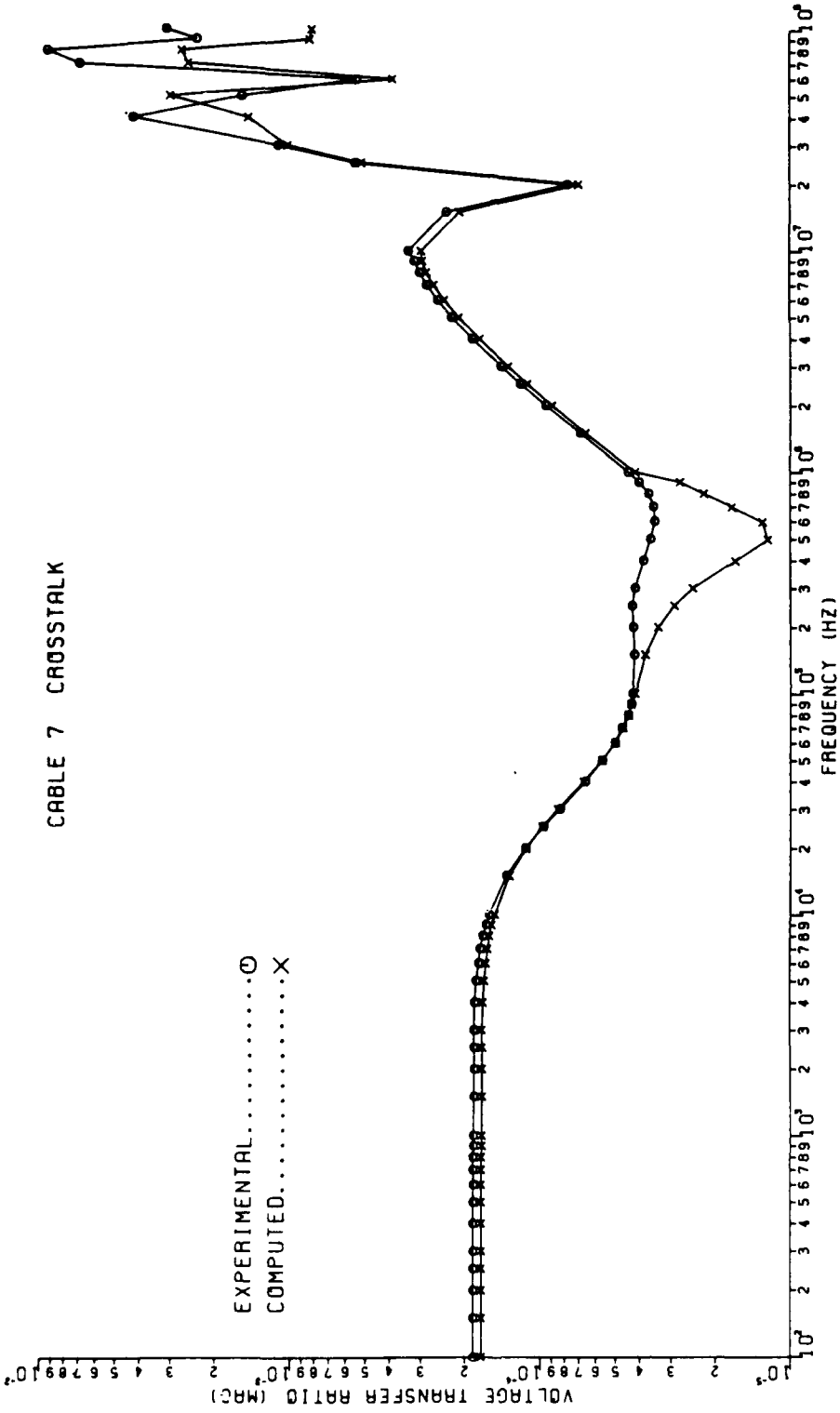

Figure 3.15 - Predicted versus Experimental Results for Cable 7.

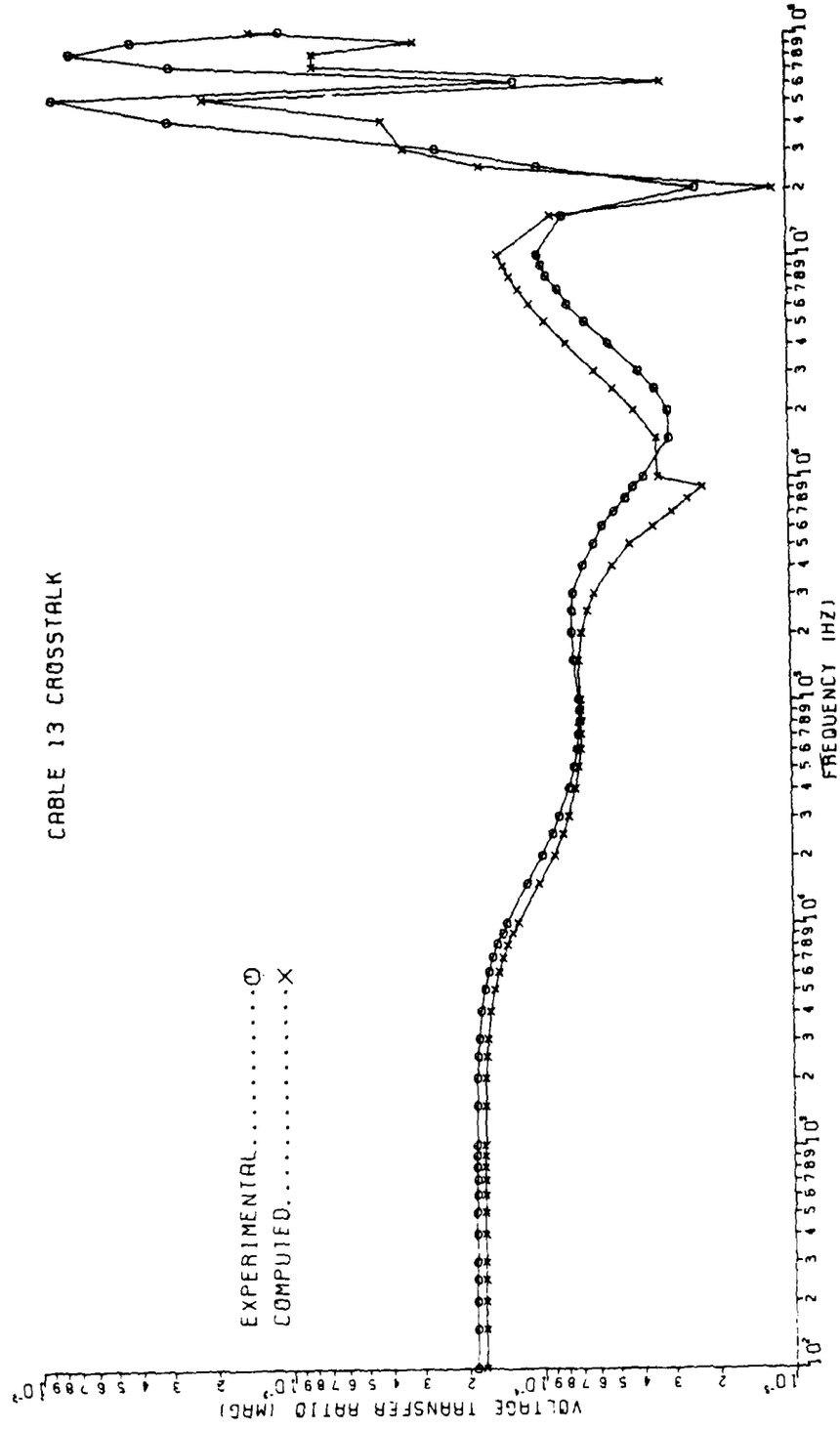

Figure 3.16 - Predicted versus Experimental Results for Cable 13.

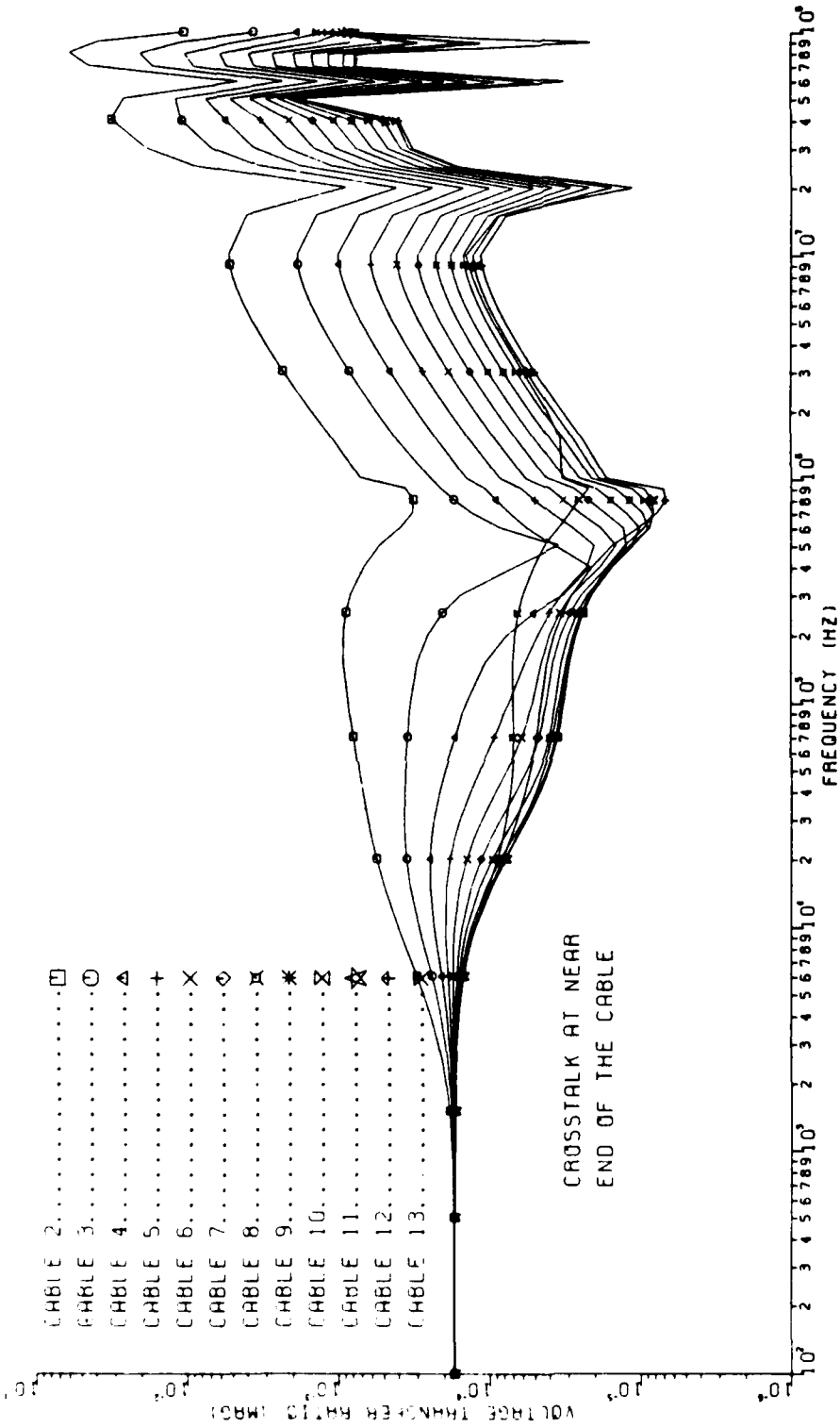

Figure 3.17 - Predictions of near-end Crosstalk.

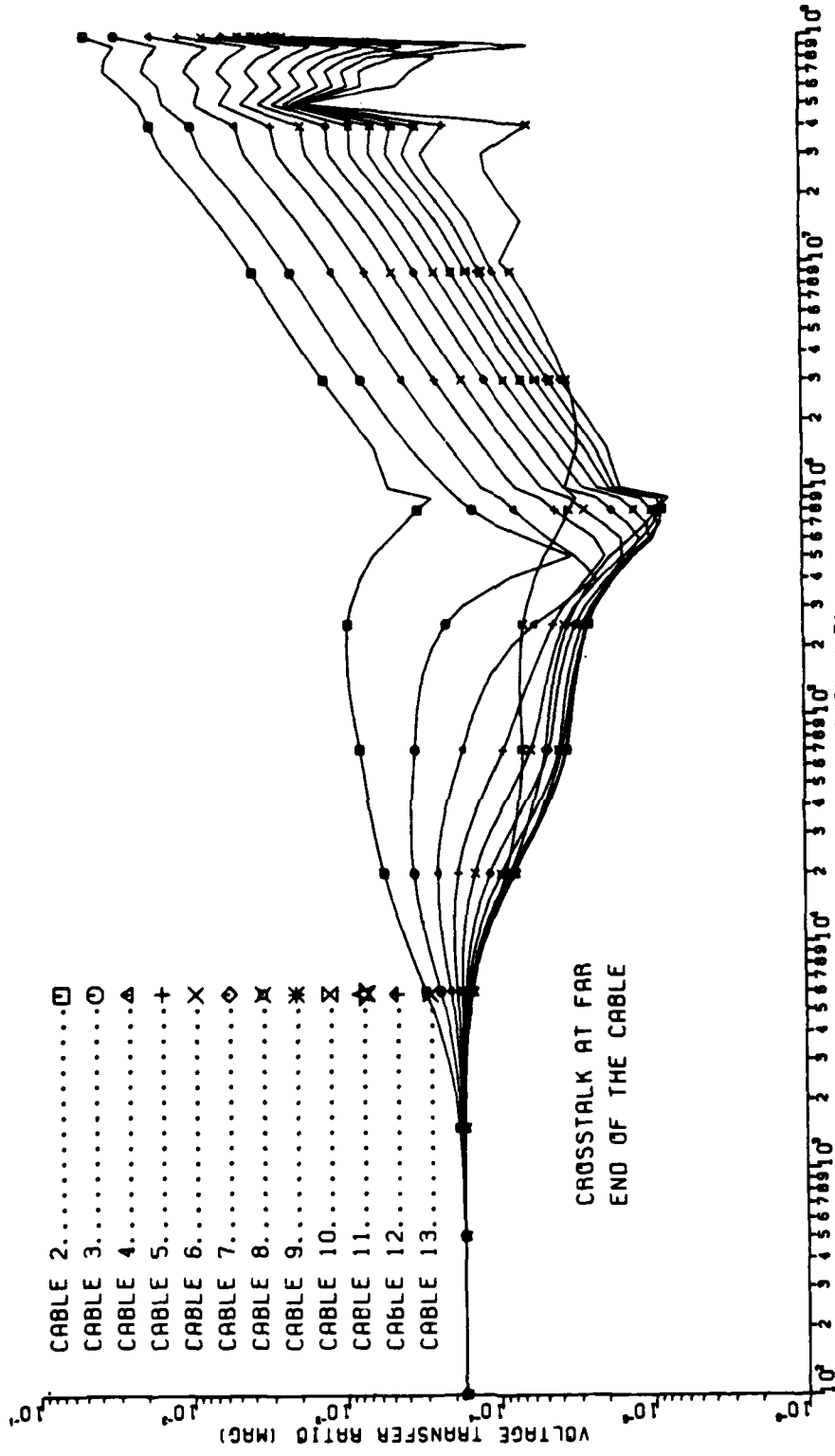

Figure 3.18 - Predictions of far-end Crosstalk.

CHAPTER 4

COMPUTER PROGRAM DESCRIPTION

Qualified requesters may obtain copies of Chapter 4 by contacting RADC (RBCT/Roy Stratton) Griffiss AFB NY 13441-5700, or calling 315-330-2563

CHAPTER 5

USERS MANUAL FOR FLATCOAX

Qualified requesters may obtain copies of Chapter 5 by contacting RADC (RBCT/Roy Stratton) Griffiss AFB NY 13441-5700, or calling 315-330-2563

CHAPTER 6

SUMMARY AND CONCLUSIONS

Crosstalk is present in almost every situation in which two or more electrical circuits are in close proximity to one another. It is often desirable to be able to predict, in advance, these levels of crosstalk for a given configuration. From these predictions a design engineer would be able to judge whether these levels of crosstalk would be acceptable in a given application. If the predicted levels were not acceptable, the cables could be "reconfigured" and the new levels of crosstalk predicted. This would point out to the designer, apriori, any configuration that will not meet the specifications given and allow for correction of the problem on paper before the system is built. Thus costly rerouting of cables or redesigning of the system may be eliminated.

A multiconductor, transmission line (MTL) model was derived in Chapter 2 to allow for this prediction of the levels of crosstalk present in a class of cables known as flatpack, coaxial cables. Predictions made with this model were compared to experimental results in Chapter 3 and were found to be very accurate. While analyzing these experimental and computed crosstalk levels, it was found that common impedance coupling due to the common grounding of the shields was the dominant contributor to the total

crosstalk at the lower frequencies. It was also found that the presence of drain wires have a significant effect on the electromagnetic coupling and, for our given configuration, actually lower the crosstalk from that which would be present without the drain wires.

It was also found that the presence of exposed, pigtail sections such as occur in plastic connectors can greatly increase the crosstalk present in a given cable at the higher frequencies. This increase was found to be on the order of 40 dB greater than if no pigtail sections were present.

The program, FLATCOAX, that was used to obtain the computed results used in Chapter 3 is listed in Appendix A with a description of its operation given in Chapter 5. Due to its accuracy in predicting experimental results we can conclude that the multiconductor transmission line model derived in Chapter 2 and implemented in this program is valid and can be used to predict levels of crosstalk present in flatpack, coaxial cables. Therefore the program can serve as a useful simulation model for design purposes.

Appendix A

FLATCOAX Program Listing

Qualified requesters may obtain copies of Appendix A by contacting RADC (RBCT/Roy Stratton) Griffiss AFB NY 13441-5700, or calling 315-330-2563

Appendix B

Conversion of FLATCOAX to Single Precision

Qualified requesters may obtain copies of Appendix B by contacting RADC (RBCT/Roy Stratton) Griffiss AFB NY 13441-5700, or calling 315-330-2563

REFERENCES

[1] C. R. Paul, "Applications of Multiconductor Transmission Line Theory to the Prediction of Cable Coupling, Volume IV, Prediction of Crosstalk in Ribbon Cables", Technical Report, RADC-TR-76-101, Rome Air Development Center, Griffiss AFB, New York, February 1978.

[2] C. R. Paul and J. W. McKnight, "Prediction of Crosstalk involving Twisted Pairs of Wires", IEEE Transactions on Electromagnetic Compatibility, Volume EMC-21, No. 2, pp. 92-114, May 1979.

[3] Dawn A. Koopman, "Modelling Crosstalk in Balanced Twisted Pairs", M.S.E.E Thesis, University of Kentucky, 1983.

[4] C. R. Paul, "Applications of Multiconductor Transmission Line Theory to the Prediction of Cable Coupling, Volume VIII, Prediction of Crosstalk Involving Braided-Shield Cables", Technical Report, RADC-TR-76-101, Rome Air Development Center, Griffiss AFB, New York, August 1980.

[5] S. A. Schelkunoff, "The Electromagnetic Theory of Coaxial Transmission Lines and Cylindrical Shields", Bell System Technical Journal, Volume 13, October 1934.

[6] S. A. Schelkunoff and T. M. Odarenko, "Crosstalk Between Coaxial Transmission Lines", Bell System Technical

Journal, Volume 16, April 1937.

[7] Saul Shenfeld, "Coupling Impedance of Cylindrical Tubes", IEEE Transactions on Electromagnetic Compatibility, Volume EMC-14, No. 1, February 1972.

[8] J. S. Hofstra, M. A. Dinallo, and L. O. Hoeft, "Measured Transfer Impedance of Braid and Convoluted Shields", IEEE EMC Symposium, 1982.

[9] L. O. Hoeft and J. S. Hofstra, "Measured Transfer Impedance of Metallized Plastic Tape and Knitted Wire Mesh Cable Shields", IEEE EMC Symposium. 1983".

[10] M. A. Dinallo, L. O. Hoeft, J. S. Hofstra, and D. Thomas, "Shielding Effectiveness of Typical Cables from 1 MHz to 1000 MHz", IEEE EMC Symposium, 1982.

[11] E. F. Vance, "Coupling to Cables", DNA Handbook Revision, Chapter 11, Stanford Research Institute, December 1974.

[12] C. R. Paul, "Applications of Multiconductor Transmission Line Theory to the Prediction of Cable Coupling", Volume I, Multiconductor Transmission Line Theory", Technical Report, RADC-TR-76-101, Rome Air Development Center, Griffiss AFB, New York, April 1976.

[13] C. R. Paul, "Effect of Pigtails on Crosstalk to Braided-Shield Cables", IEEE Transactions on Electromagnetic Compatibiliity, Volume EMC-22, No. 3, August 1980.

[14] AMP Coaxial Ribbon Cable Assemblies, Cable and Connectors, Catalog 75-342, Revised 8-81, AMP Incorporated, Harrisburg, PA.

[15] IMSL (International Mathematical and Statistical Library), IMSL, Inc. GNB Building, 7500 Bellaire Blvd., Houston, Texas 77036.

[16] Private communication with Dr. Lothar O. Hoeft of the BDM Corporation, Albuquerque, NM.

MISSION
of
Rome Air Development Center

RADC plans and executes research, development, test and selected acquisition programs in support of Command, Control Communications and Intelligence (C^3I) activities. Technical and engineering support within areas of technical competence is provided to ESD Program Offices (POs) and other ESD elements. The principal technical mission areas are communications, electromagnetic guidance and control, surveillance of ground and aerospace objects, intelligence data collection and handling, information system technology, ionospheric propagation, solid state sciences, microwave physics and electronic reliability, maintainability and compatibility.

END

FILMED

5-85

DTIC